Identification and characterization of a ubiquitin E3 RING ligase of the *Chlamydia*-like bacterium *Simkania negevensis*

Eva-Maria Hörner[1], Vanessa Boll[2], Thomas Hermanns[2], Adriana Moldovan[1], Kay Hofmann[2], Vera Kozjak-Pavlovic[1, *]

(1) Chair of Microbiology, Biocenter, Julius-Maximilian University Würzburg, D-97074 Würzburg, Germany.

(2) Institute for Genetics, University of Cologne, Zülpicher Straße 47a, D-50674 Cologne, Germany

* Corresponding author: Vera Kozjak-Pavlovic; Biocenter, Am Hubland, D-97074 Würzburg, Germany; vera.kozjak@uni-wuerzburg.de

Running title: E3 RING ligase from *Simkania negevensis*

Keywords: RING ligase, Simkania negevensis, Chlamydia, ubiquitin, intracellular bacteria, infection

Abstract

In the arms race between a pathogen and the host, many bacteria have acquired a sizable armory to counteract or change the defense mechanisms of the host cell, including the eukaryotic ubiquitin system. *Simkania negevensis*, an obligate intracellular *Chlamydia*-like bacterium, is one such example. *S. negevensis* has a biphasic developmental cycle, similar to other members of the *Chlamydiales* order. The bacterium develops inside a tubular membranous compartment called *Simkania*-containing vacuole, which is in close contact with the host endoplasmic reticulum (ER) and mitochondria. It can infect a wide range of hosts, with a long infection cycle lasting up to 15 days, and is associated with respiratory tract diseases. Recently, *S. negevensis* has been discovered to possess an unusually large number of deubiquitinating enzymes, but not much is known about the variety of other ubiquitin-modifying enzymes in this bacterium. Our study provides an initial description of the activity of a so far uncharacterized *S. negevensis* ubiquitin E3 RING-ligase (SNE_A12920 or SneRING). We report that SneRING primarily generates K63- and K-11 linked ubiquitin chains and preferentially interacts with UbcH5b and UBE2T E2 ubiquitin ligases among the ones we tested. Bacteria express SneRING upon infection of various human cell lines, as well as amoeba. In addition, we demonstrate that a portion of the expressed SneRING co-localizes with mitochondria and ER. Mass spectrometry studies of the SneRING interactome show enrichment in mitochondrial and ER proteins containing a prohibitin domain and involved in organelle morphology, respiration, and stress response. Our work offers the first insights into the function of an *S. negevensis* RING ligase, an enzyme potentially involved in organelle remodeling to accommodate the unique lifestyle of this intracellular bacterium.

Introduction

Simkania negevensis (Sne) is an obligate intracellular *Chlamydia-like* bacterium, first described in 1993 as a cell culture contaminant of unknown origin (Kahane *et al*, 1993). Based on sequence comparison of the ribosomal DNA (rDNA), it has been classified as a member of the family *Simkaniaceae* within the order *Chlamydiales* (Everett *et al*, 1999). The bacterium survives and replicates in a great variety of hosts ranging from different eukaryotic cells including immune cells such as macrophages (Kahane *et al*, 2008; Kahane *et al*, 2007) to arthropods (Croxatto *et al*, 2014) and amoeba (Kahane *et al*, 2001). However, its natural host is unknown. Sne has been associated with different infections of the respiratory tract, including acute bronchiolitis in infants (Kahane *et al*, 1998) and community-acquired pneumonia (Lieberman *et al*, 1997). Furthermore, patients positive for Sne had a higher risk of transplanted lung rejection (Husain *et al*, 2007; Jamal *et al*, 2015). In addition, Sne has been also connected to Crohn´s disease (Scaioli *et al*, 2019). However, recent studies dispute the link between Sne and respiratory tract infections (Al-Younes *et al*, 2017). While

62 some of the closely related *Chlamydia*-species, such as *Chlamydia trachomatis*, the causative agent of
63 sexually transmitted disease and trachoma (Newman *et al*, 2015), or *Chlamydia pneumoniae*, which
64 causes acute respiratory diseases (Kuo *et al*, 1986), are highly pathogenic, it remains unclear to what
65 extend Sne can cause infections in immunocompetent individuals.

66 Like other members of the *Chlamydiales*, Sne exhibits a biphasic developmental cycle, which is
67 characterized by the alternating differentiation into two forms. While Reticulate Bodies (RB)
68 represent the large, replicative, metabolically active intracellular form, which is stained
69 homogeneously, the infective smaller and electron-dense form resembles the environmental
70 Elementary Bodies (EB) of *Chlamydia* (Kahane *et al.*, 1993; Kahane *et al*, 2002). Inside the host cell,
71 Sne replicates within a *Simkania*-containing vacuole (SnCV). The SnCV is a membranous, tubular
72 system that is associated with mitochondria and forms extensive contact sites with the endoplasmic
73 reticulum (ER) of the host cell (Mehlitz *et al*, 2014). Sne exhibits a significantly longer life cycle than *C.*
74 *trachomatis*. SnCV development and number of RBs plateau on day 3 post-infection (pi). An increased
75 release of Sne infectious particles from infected HeLa or differentiated THP-1 cells starts on day 4 or
76 day 5 pi, respectively (Koch *et al*, 2020), which is longer than the usual 2-3 days for *C. trachomatis*
77 (Jury *et al*, 2023). In addition, Sne-infected cells can be observed in culture for up to 15 days (Kahane
78 *et al.*, 2002).

79 Given that bacteria proliferating within the host cell are exposed to the host cytoplasm, they risk
80 being targeted by the cell-autonomous immunity. This includes the ubiquitination of free-living
81 bacteria as well as bacteria that live in specialized vacuoles (Hermanns & Hofmann, 2019).
82 Ubiquitination is a dynamic, versatile protein modification that regulates various cellular aspects in
83 eukaryotes. The covalent attachment of ubiquitin to the targeted protein occurs through a cascade
84 with three different enzymes: the E1 ubiquitin-activating enzyme, the E2 ubiquitin-conjugating
85 enzyme, and the E3 ubiquitin-ligating enzyme. During ubiquitination, a single ubiquitin molecule is
86 attached to a lysine residue of a specific substrate through an isopeptide bond. The complexity of
87 ubiquitination is further increased by the property of ubiquitin itself to become ubiquitinated at one
88 or more of its seven lysine residues, giving rise to ubiquitin chains. In addition, also the N-terminus of
89 ubiquitin can be modified, which results in the possibility of forming eight different linkage types
90 (Swatek & Komander, 2016).

91 Depending on the type of the ubiquitin chain, the outcome for the modified substrate differs. The
92 prototypical ubiquitin chains are linked by lysine (K) 48 or 63 of the ubiquitin moieties. While K48-
93 linked ubiquitin chains target their substrate for proteasomal degradation, K63-linked ubiquitin chains
94 regulate NF-kB transcription factor activation, responses of the immune system, repair of DNA,
95 sorting of proteins, clearance of damaged mitochondria and they can also control the assembly of

96 large protein complexes that drive translation or splicing of mRNA. Ubiquitin chains, connected via
97 the free N-terminus or the remaining five lysine residues are said to be atypical conjugates. These
98 include K11-, K6-, and M1-linked ubiquitin chains. K-11 linked chains play a role during cell division by
99 targeting cell cycle regulators for degradation. Interestingly, K11-conjugates are also associated with
100 innate immune response against viruses (Yau & Rape, 2016). Although not much is known about the
101 cellular function of K6-linked ubiquitin chains, they have been observed to accumulate upon
102 depolarization of mitochondria and after UV radiation. Ubiquitin moieties linked via their free N-
103 terminus, also referred to as linear or M1-linked ubiquitin chains, are involved in the regulation of
104 immune response and inflammation through regulating the activation of the NF-kB transcription
105 factor (Akutsu *et al*, 2016).

106 A recent discovery of branched and mixed ubiquitin chains forms another level of ubiquitination
107 diversity. Determining the function of branched polymers is challenging but gives new insights into
108 the variety of information that can be transported by ubiquitin signals. K11/K48 heterotypic ubiquitin
109 chains are assembled during mitosis and on misfolded proteins in the ER or cytoplasm. They have
110 been shown to play a role in cell cycle control, enhance substrate recognition, and accelerate
111 proteasomal degradation. In contrast, branched K48/K63 conjugates are synthesized in response to
112 the activation of the transcription factor NF-kB. Additionally, modification of substrates during
113 apoptotic response with this mixed chain type results in their degradation by the proteasome (French
114 *et al*, 2021; Haakonsen & Rape, 2019). For mixed K11/K63-linked polymers, a non-proteolytic function
115 during endocytosis and signaling via the transcription factor NF-kB has been determined (Wickliffe *et*
116 *al*, 2011). Even though K6/K11 and K6/K48 branched ubiquitin chains have already been identified,
117 their functions remain unclear (Haakonsen & Rape, 2019).

118 Based on their structure and mechanism of ubiquitin transfer, E3 ubiquitin ligases are usually divided
119 into three classes: RING (really interesting new gene), RBR (RING-between-RING), and HECT
120 (homologous to the E6/AP carboxyl terminus) ligases. While RBR and HECT E3s form a catalytic
121 intermediate with ubiquitin by binding the ubiquitin from the loaded E2 enzyme to themselves
122 before conjugating it to the target protein, RING ligases directly transfer ubiquitin from the E2
123 enzyme to the substrate (Toma-Fukai & Shimizu, 2021). With more than 600 RING ligases encoded by
124 the human genome, this group is the largest. RING E3s are characterized by a RING domain that
125 directly binds the substrate and the ubiquitin-loaded E2 enzyme. By bringing both components into
126 proximity, RING ligases catalyze ubiquitin transfer from the conjugating enzyme to the target protein
127 (Deshaies & Joazeiro, 2009; Zheng & Shabek, 2017).

128 Many pathogenic bacteria have acquired a sophisticated range of effectors, including ubiquitin E3
129 ligases, to exploit the host cell's ubiquitin system for their benefit. Examples include SopA, a HECT-like

130 E3 ligase from *Salmonella*, LubX, a RING-like E3 ligase from *Legionella*, as well as several novel E3
131 ligases from *Shigella* (Maculins *et al*, 2016). By ubiquitinating the substrates, they modify the
132 ubiquitin code to form a niche that allows them to survive and multiply within the host cell (Dikic &
133 Schulman, 2023).

134 Since Sne is capable of long infections and intracellular growth while simultaneously efficiently
135 suppressing the host defense system, it is of great interest how the bacterium accomplishes this.
136 Recent studies showed that Sne possesses an unusually high number of deubiquitinating enzymes
137 (DUBs) with sometimes interesting cleavage specificities. Furthermore, these DUBs are from diverse
138 classes, of which some have never been described in bacteria (Boll *et al*, 2023).

139 In this work, we focused on identifying and characterizing putative ubiquitin (E3) RING ligases of Sne.
140 We focused on a RING ligase Sne_A12920 (SneRING), a 25.4 kDa protein containing an unusual RING
141 finger when compared to other bacterial RING ligases. We purified the enzyme and determined its
142 ubiquitinating activity, as well as detected the region of interaction with the E2 ubiquitin-conjugating
143 enzyme. Additionally, we demonstrated that the SneRING shows different ubiquitination activity
144 depending on the E2 conjugating enzyme it interacts with. Finally, we determined that the ligase
145 generates specific types of ubiquitin chains, rather than producing all chain types. SneRING is
146 expressed in different human cell lines as well as in amoeba during infection. After expression in
147 human cells, a portion of the protein is associated with the ER and mitochondria. The possible
148 interaction partners of SneRING include mitochondrial and ER proteins that play a role in morphology,
149 energetics, and transport, indicating the potential mode of action of this bacterial enzyme. Taken
150 together, our data provide first insights into the previously unknown world of ubiquitin ligases in
151 *Simkania negevensis*.

152

153 ## Results

154 **Identification of RING ligases in *Simkania negevensis***

155 To identify ubiquitin ligase candidates in the sequenced genome of Sne (Collingro *et al*, 2011), the Sne
156 subset of UniProt (UniProtConsortium, 2023) was searched with generalized profiles (Bucher *et al*,
157 1996) representing classical RING finger domains and several RING finger variants. When using a
158 profile derived from a multiple alignment of established RING domains, only a single Sne ORF,
159 Sne_A12920 (SneRING), reached a significant score of $p<0.01$. To validate this finding, BLAST and
160 profile searches were used to find other bacterial proteins related to SneRING. A small family was
161 identified, of which representative members include Sim-KFB93 and Sim-QNJ27 from bacteria
162 belonging to the *Simkaniaceae* family, and Chl-HKST.2, belonging to an unclassified *Chlamydiia* (Fig

163 1A). An Alphafold (Jumper *et al*, 2021) model of SneRING shows a two-domain architecture with a
164 RING-like fold forming the first domain (residues 14-72), followed by a linker region and a C-terminal
165 α/β-fold domain without informative sequence or structural similarities (Fig 1B). Like canonical RING
166 fingers, the RING-like domain of SneRING is predicted to coordinate two Zn^{2+} ions, albeit using
167 somewhat atypical ligand residues. In the model, the first Zn^{2+} ion is coordinated by Cys-17, Cys-20,
168 His-40, and Cys43, while the second Zn^{2+} ion is contacted by Asn-32, Cys-35, Cys-54, and Cys57.

169 A DALI (Holm, 2022) search using the RING-like region of SneRING identified as significant top-hits the
170 established RING fingers of TRIM37 (pdb:3LRQ, Z-score 9.1) and RING2 (pdb:6WI7, Z-score 8.9).
171 RING2 possesses a typical RING finger, where Zn_1 is coordinated by two CxxC dyads and Zn_2 is bound
172 by a CxH and a CxxC dyad. In SneRING, both coordination spheres are slightly altered: His-40 replaces
173 Cys as the 3rd ligand of Zn_1, while the first two ligands of Zn_2 are NxxC rather than the canonical CxH
174 (Fig 1A). Functionally, these changes might be inconsequential, as Alphafold model of the
175 Sne_A12920 RING domain in contact with UbcH5 predicts SneRING to form a complex with E2
176 enzymes resembling that of other RING ligases (Fig 1C). As with other RING fingers, the most
177 important contacts are made by the region surrounding the first Zn-binding dyad. While most other
178 RING domains contact E2s by a conserved hydrophobic residue before the 2nd Zn-binding cysteine,
179 SneRING carries the atypical Ser-19 at this position, which does not form a specific E2 interaction in
180 the model. Instead, Glu-22 forms short-distance salt bridges to Lys-4 and Lys-8 of UbcH5 (Fig 1C). We
181 reasoned that a mutation of Glu-22 combined with a Ser-19 mutant might abrogate E2-binding.
182 Indeed, when subjecting an S19R_E22R variant of SneRING to Alphafold modeling with UbcH5, no
183 productive complex was formed.

184 Besides the significantly-scoring SneRING, three further RING-like domains could be identified
185 bioinformatically. A closer inspection of the borderline-significant matches identified the
186 uncharacterized ORF Sne_A08700 and its close relative (and genomic neighbor) Sne_A08690 to have
187 a conspicuous arrangement of cysteine and histidine residues. The assumed RING-relationship of
188 these two proteins is supported by the conservation pattern of their sequence family and by
189 Alphafold modeling: Sne_A08700 is predicted to use eight canonical ligands for coordinating two Zn^{2+}
190 ions (Fig S1A); the best DALI match to an established RING-finger was RNF125 (pdb:5DKA, Z-score
191 5.6). Sequence conservation between RNF125 and the Sne_A08700 family shows a big insertion after
192 the 3rd Zn ligand (Fig S1B), which explains the poor score in the initial profile search. The closely
193 related protein Sne_A08690 has lost three ligands for the first Zn^{2+} ion and probably coordinates only
194 a single ion. A 4th RING candidate (Sne_A19470) was picked up in profile searches using the SP-RING
195 family, a subgroup of RING-like domains usually involved in SUMO conjugation (Hochstrasser, 2001).
196 However, a closer inspection suggested that Sne_A19470 does not contain an SP-RING domain but
197 rather a (degenerate) conventional RING that has lost its ligands for Zn_1 coordination (Fig S1C). The

198 best DALI matches were TRIM69 (pdb:6YXE, Z-score 8.5) and TRIM2 (pdb:8A38, Z-score 8.3), which
199 both contain a structurally similar RING domain, but with a complete set of eight ligand residues (Fig
200 S1D).

201 Considering that SneRING was the only protein with a RING-like domain that has been identified in a
202 previously published proteomics analysis of the ER/SnCV membrane of infected HeLa229 cells on day
203 3 pi (Herweg *et al*, 2016), we focused on further characterization of this enzyme.

204

205 **SneRING is an active E3 RING ligase with an E2 enzyme-interacting region within its predicted RING**
206 **domain.**

207 Our bioinformatic analysis only predicts putative RING ligases without hinting at the protein function.
208 Therefore, we first tested the activity of the SneRING by analyzing ubiquitin chain assembly during an
209 *in vitro* autoubiquitination assay. To do so, we purified SneRING and incubated it with a ubiquitin-
210 activating (E1) and a ubiquitin-conjugating enzyme (E2) as well as free ubiquitin and ATP to allow the
211 enzyme cascade to covalently attach ubiquitin to SneRING. Already after 30 min of incubation, we
212 could detect a strong ubiquitin signal that increased over time, while in the negative control without
213 SneRING, only monoubiquitin could be detected (Fig 2A). This indicates that the SneRING is an active
214 ubiquitin ligase.

215 Since Alphafold modeling indicated the importance of Glu-22 and Ser-19 for the interaction with an
216 E2 enzyme, we replaced these two amino acids with arginine to generate a catalytically inactive form
217 and performed an *in vitro* autoubiquitination assay with the purified mutated enzyme for 5 h. While
218 in the presence of the wild-type SneRING a strong ubiquitin signal could be detected, no ubiquitin
219 chains were formed in the reaction containing SneRING S19R_E22R (Fig 2B). This confirms that the N-
220 terminal domain of the SneRING interacts with the E2 ubiquitin-conjugating enzyme and is necessary
221 for the enzyme function.

222 To test whether SneRING can generate ubiquitin chains when combined with other E2 enzymes
223 besides UbcH5b, we performed an *in vitro* autoubiquitination assay for 5 h using selected ubiquitin-
224 conjugating enzymes. Only UbcH5b- and, to a lesser extent, UBE2T-containing reactions showed the
225 presence of the poly-ubiquitin signals, while no ubiquitin chain assembly occurred with the addition
226 of the E2 enzymes UbcH7, UBE2A, and UBE2W (Fig 2C). The time course analysis of the
227 autoubiquitination reaction in combination with UbcH5b showed strong ubiquitination after 30 min
228 of incubation, increasing over time (Fig 2A,D). In contrast, in the presence of UBE2T nearly no
229 reaction was observed after 30 min, while 2 h and 5 h later, some poly-ubiquitin signal was
230 detectable (Fig 2D). Among the tested E2 enzymes, SneRING appears to be most active in

231 combination with UbcH5b, while a moderate reaction also occurs together with the ubiquitin-
232 conjugating enzyme UBE2T.

233

234 **Ubiquitin chains generated by SneRING are cleaved by deubiquitinating enzymes specific for the**
235 **K11/K63 linkage type.**

236 To characterize the type of ubiquitin chains formed by SneRING, we performed linkage-specific chain-
237 cleaving assays (UbiCRest assays) (Hospenthal *et al*, 2015). Ubiquitin chains generated by SneRING
238 after *in vitro* autoubiquitination for 5 h were incubated with a panel of different DUBs that either
239 process any chain type, such as ubiquitin-specific peptidase 21 (USP21) (Ye *et al*, 2011), or have
240 specificity against certain ubiquitin chain linkages. When incubating the reaction with the USP21, no
241 remaining polyubiquitin signal could be detected. Treatment with the K11-specific DUB Cezanne
242 (Bremm *et al*, 2010) or with the K63-specific DUB AMSH (associated molecule with an Src homology 3
243 domain of signal transducing adaptor molecule, STAM) (Komander *et al*, 2009), strongly reduced the
244 polyubiquitin signal. In contrast, no cleavage was observed upon incubation with the DUB SneOTU
245 that specifically cleaves linear M1 ubiquitin chains or SneVTD that shows cleavage specificity against
246 K6-linked ubiquitin chains (Boll *et al.*, 2023). Furthermore, also the K48-specific DUB OTUB1 (Wang *et*
247 *al*, 2009) did not visibly reduce the ubiquitin signal (Fig 3A).

248 To test whether the ligase only generates these two linkage types, or if other ubiquitin chain types are
249 produced at a lower level, a di-UbiCRest assay was performed. To do so, next to incubating an *in vitro*
250 SneRING autoubiquitination reaction with the K11- specific DUB Cezanne or with the K63- specific
251 DUB AMSH, the reaction was also incubated with both enzymes simultaneously. As already observed,
252 Cezanne and AMSH led to a reduction of the ubiquitin signal, demonstrating the presence of K11- and
253 K63-linked ubiquitin chains. However, the combined activity of both DUBs did not completely
254 degrade the ubiquitin chains generated by the SneRING (Fig 3B), indicating that other linkage types
255 are formed by the SneRING in addition to K11- and K63-linked ubiquitin chains. Mass spectrometry of
256 the *in vitro* SneRING autoubiquitination reaction in the presence of UbcH5b (UBE2D2) mainly
257 detected K11- and K63-linked GlyGly-modified peptides, with some signals for K6- and K48-modified
258 peptides also visible. Similar results with overall weaker signal strength were obtained for the
259 reaction containing the E2 enzyme UBE2T (Fig 3C). In conclusion, SneRING forms *in vitro* mostly K11-
260 and K63-, in addition to K6- and K48-linked ubiquitin chains.

261 To further validate this finding, *in vitro* autoubiquitination assays performed with UbcH5b were
262 tested by immunoblot analysis for the presence of specific ubiquitin chains. We detected strong
263 signals using antibodies against K11- (Fig S2A) and K63-linked chains (Fig S2B). For K6- and K48-linked

264 chains we used native linked di-Ubiquitin conjugates as positive controls (UbiQ). The antibody
265 against K48-linked ubiquitin chains produced a signal in the control sample, as well as in the ubiquitin
266 chains generated by SneRING (Fig S2C). Similar observations were made when using an antibody
267 against K6-linked ubiquitin conjugates (Fig S2D). However, when we used an antibody against M1-
268 linkages, which were not detected by UbiCRest assay and mass spectrometry, we only saw a signal in
269 the positive control, but not in the SneRING reaction, confirming the previous results (Fig S2E).

270

271 **SneRING is expressed during infection of human cells and its possible natural host *Acanthamoeba***
272 ***castellanii***

273 We next analyzed the expression pattern of SneRING during infection. Since Sne can infect and grow
274 in a variety of cells (Vouga *et al*, 2017), as well as survive and multiply within *Acanthamoeba*
275 *castellanii*, we measured the SneRING mRNA levels during the infection cycle of various cell lines and
276 amoeba by RT-qPCR analysis and normalized it against the mRNA level of the bacterial 5S RNA. In
277 comparison, we measured the mRNA levels of a highly-expressed gene, Sne chaperone SnGroEL.
278 SneRING was expressed in all host cells we tested, though to a lesser extent than SnGroEL (Fig S3).
279 Expression intensities of SneRING in different human cell lines were comparable. In HeLa229 and
280 U2OS cells we observed somewhat higher SneRING expression on day 2 pi compared to day 4 pi (Fig
281 S3A,B).

282 Sne can infect and grow in macrophages (Kahane *et al.*, 2008), as well as in the THP-1 cell line that
283 mimics the macrophage-like state after differentiation by PMA (Chanput *et al*, 2014), in contrast to *C.*
284 *trachomatis* (Herweg & Rudel, 2016). We analyzed and compared the expression of SneRING in the
285 THP-1 cell line and primary human M2-like macrophages. Based on the observation that infective Sne
286 particles can be detected on day 6 pi in macrophages (Kahane *et al.*, 2008), we included this time
287 point in our experimental setup. RT-qPCR analysis showed slightly higher expression of SneRING in
288 THP-1 cells than in M2-like macrophages. There were no notable differences in the mRNA levels
289 between different days pi (Fig S3C,D).

290 By taking up a high number of bacteria, many free-living protozoa mimic the role of professional
291 phagocytes (Fritsche *et al*, 2000). Sne can survive and grow within amoeba (Kahane *et al.*, 2001).
292 Since Sne establishes a long-term infection in amoeba, we measured the mRNA level of SneRING only
293 on day 4 pi. *A. castellanii* culture was cultivated at 30 °C instead of 37 °C that we used for cultivation
294 of human cell lines (or 35 °C for Sne infected). mRNA of SneRING was detectable, but the levels varied
295 strongly between the samples both for SneRING and SnGroEL (Fig S3E).

296

297 **SneRING localizes to host cell cytoplasm, mitochondria, and ER after overexpression, associating**
298 **with the inner mitochondrial membrane**

299 We next studied the localization of SneRING in the host cell. Since we were unsuccessful in producing
300 an antibody against SneRING that would recognize the native protein, we limited our studies to the
301 FLAG-tagged protein we expressed from a plasmid in U2OS cells. To increase the efficacy of SneRING
302 expression, we used a human codon-adjusted version of the gene. SneRING was successfully
303 expressed and exhibited cytosolic distribution as observed by immunofluorescence microscopy (Fig
304 4A). The FLAG-tagged protein could also be identified by western blot after transfection (Fig 4B).
305 Upon subcellular fractionation and separation of the cells into the crude mitochondrial, the light
306 membrane, and the cytosolic fraction, SneRING signal was distributed between all fractions (Fig 4C).
307 In comparison, Mic60, a mitochondrial inner membrane protein, localized almost exclusively to
308 mitochondrial fraction, while calnexin, the integral protein of the ER, was detected in both the light
309 membrane and the crude mitochondrial fraction. GAPDH and tubulin were associated with every
310 fraction but mainly localized in the cytosol, somewhat resembling SneRING distribution (Fig 4C).

311 Immunofluorescence microscopy of HeLa229 cells with GFP-labeled mitochondria (Fig S4A) or dsRED-
312 labeled ER (Fig S4B) that were transfected with FLAG-tagged SneRING gave a similar picture, with
313 some overlap of the signal, indicating possible association of SneRING with these organelles. This did
314 not significantly change upon infection with Sne (Fig S4A,B, lower panels). Notably, Sne-infected cells
315 show fragmentation of the mitochondria, which is absent in cells transfected only with SneRING. In
316 both cell lines, the FLAG-tagged protein is pushed to the cell periphery with the cytosol and is not
317 identified in the SnCV when the cells are infected (Fig S4).

318 The observed association of SneRING with mitochondria could be caused by the interaction with the
319 mitochondrial surface or result from the insufficient purity of the mitochondrial fraction, which
320 contains ER and contaminations from other cellular compartments. To analyze this further, we
321 isolated mitochondria from the FLAG-SneRING-transfected U2OS cells and subjected them to swelling
322 in a hypotonic buffer in the absence or the presence of Protease K (PK). The accessibility of the
323 proteins to PK demonstrates their submitochondrial localization. As a positive control, mitochondria
324 were completely solubilized by 1% Triton X-100 and treated with PK (Fig 4D). Surprisingly, FLAG-
325 tagged SneRING could be detected even after PK treatment of intact mitochondria, indicating that the
326 protein is not localized on the mitochondrial surface. In contrast, Tom70, a mitochondrial outer
327 membrane protein, is degraded under similar conditions, comparable to the ER protein calnexin.
328 Opening of the outer membrane by swelling leads to a partial release of an intermembrane-space
329 protein coproporphyrinogen oxidase (CPOX), but the inner membrane protein Mic60, the matrix
330 protein Tim44, and SneRING remain undisturbed. PK treatment of the mitochondria with the

331 ruptured outer membrane leads to a degradation of CPOX as well as Mic60, which is exposed to the
332 intermembrane space, while Tim44 is degraded completely only after complete solubilization of
333 mitochondria by a detergent. SneRING behaves in this respect like Mic60 since most of the protein is
334 degraded upon PK treatment of swollen mitochondria. A small portion of the protein, however,
335 remains undigested, indicating possible protection by the inner mitochondrial membrane (Fig 4D).

336 We performed carbonate extraction of isolated mitochondria using 100 mM Na_2CO_3, pH 11.5 or pH
337 10.8 to assess membrane integration of SneRING. In addition, the membrane association of the
338 protein was tested by sonicating mitochondria in a high salt buffer. Hsp60, a soluble mitochondrial
339 matrix protein, was found in both pellet and supernatant fractions after milder carbonate extraction
340 and extraction in the high-salt buffer but was fully extracted at pH 11.5. In contrast, Sam50, an
341 integral protein of the outer mitochondrial membrane, was only detected in the pellet after
342 treatment in all three conditions. Mic60, the transmembrane protein of the inner mitochondrial
343 membrane, was partially extracted from membranes only after carbonate extraction at the higher pH
344 of 11.5. FLAG-tagged SneRING was detected in both the pellet and the supernatant after incubation
345 in all three conditions, suggesting that the protein is mostly membrane-associated. A small portion,
346 however, appears to be a membrane-integral protein (Fig 4E). We conclude that a portion of SneRING
347 localizes to the host cell mitochondria after overexpression. The protein is most likely associated with
348 the inner mitochondrial membrane.

349

350 **Putative SneRING-ligase interacting partners include mitochondrial and ER proteins involved in the**
351 **regulation of organelle morphology, transport, and energetics**

352 To determine possible host cell targets of SneRING, we expressed the FLAG-tagged protein in U2OS
353 cells with and without Sne infection and performed a pull-down using FLAG-antibody followed by
354 mass spectrometry analysis. We compared infected samples with and without ectopically expressed
355 FLAG-tagged SneRING to determine significantly enriched proteins (Fig 5A). Highly enriched proteins
356 (log2 fold change > 2) included mitochondrial proteins involved in organelle morphology (prohibitins,
357 Mic60/IMMT), oxidative phosphorylation (OXPHOS) (subunits of ATPase and respiratory chain
358 components), as well as transport (VDAC1 and 2). However, several ER proteins were also identified,
359 and these included ER-microtubule anchoring protein CKAP4, BCAP31, a protein involved in ER-
360 associated degradation (ERAD) and acting as an ER stress sensor that mediates communication with
361 mitochondria (Namba, 2019), and ERLIN1 and 2, which are prohibitin-domain containing proteins
362 involved in ERAD (Pearce *et al*, 2009) (Fig 5A, Table S1).

363 Besides these cellular proteins, a number of *Simkania*-derived proteins were also strongly enriched in
364 the SneRING-pulldowns (Fig S5, Table S1). These proteins might be bacterial SneRING targets or co-
365 factors of SneRING. None of the top-enriched Sne proteins appears to be experimentally
366 characterized, but several members of this set have informative sequence relationships. SNE_A02810,
367 SNE_A02800, SNE_A02780, SNE_A18120, and SNE_A05090 are relatives of the *Legionella* major
368 outer membrane protein mOMP, and SNE_08170 contains mOMP-associated POTRA domains. Other
369 enriched proteins are related to components of bacterial secretion systems: A21850 is related to the
370 SecDF secretion protein, SNE_A20110 is related to the T2SS secretin GspD, while SNE_A10070 is
371 related to bacterial signal peptidases. Overall, the bacterial SneRING-associated proteins appear to be
372 located at the bacterial surface.

373 When comparing the cellular SneRING-associated proteins of Sne-infected and non-infected cells, a
374 very similar set of proteins was obtained. The top fourteen cellular infection-specific SneRING
375 interactors were found also on the previous list. We again found mitochondrial and ER proteins
376 among the hits. Interestingly, GOLIM4, a protein localized to Golgi apparatus and playing a role in
377 endosome to Golgi protein transport (Natarajan & Linstedt, 2004), was also found as one of the most
378 highly enriched proteins in both lists (Fig 5B, Table S1). Taken together, these results show clustering
379 of putative SneRING targets in groups of ER and mitochondrial proteins functioning in quality control,
380 bioenergetics, and morphology. The localization of these targets is in agreement with the possible
381 localization of SneRING that we previously determined (Fig 4). The observation that most of the
382 prominent SneRING interactors are only present in the infected samples suggests that SneRING needs
383 additional bacterial factors for its function, or that the infection-induced remodeling of cellular
384 compartments fosters SneRING interactions.

385

386 ## Discussion

387 After invading the host cell, intracellular bacteria reside either directly within the cytosol or inside a
388 vacuole. In both cases, they are targeted by the innate immune system of the host cell to induce their
389 clearance and block their propagation. To survive and replicate, intracellular pathogens must modify
390 and/or evade the host defense system. An important part of intracellular defenses is the ubiquitin
391 system.

392 Ubiquitin system has been thought to be exclusive to eukaryotes; however, recent reports about
393 bacterial ubiquitination systems that serve as anti-viral defense show that ubiquitination might be
394 evolutionarily older than presumed (Chambers *et al*, 2024; Hör *et al*, 2024). In addition, various
395 bacteria specifically counteract their ubiquitination and even hijack the system for their own

396 advantage by secreting effector proteins (Tripathi-Giesgen *et al*, 2021). Thus, the ubiquitin system of
397 the host cell represents a weapon for both the host cell and the bacteria. Bacterial DUBs can prevent
398 bacterial ubiquitination, which can be a signal for xenophagy (Chai *et al*, 2019; Otten *et al*, 2021;
399 Yamada *et al*, 2021). Furthermore, some bacteria deliver unique virulence factors that functionally
400 mimic mammalian E3 ligases to exploit the host ubiquitin system. Ubiquitin E3 ligases of all three
401 types have been described for various bacteria. These differ in their target in the host cell and their
402 intracellular function (Ashida & Sasakawa, 2017).

403 Recent studies have shown that *S. negevensis* possesses a high number of DUBs from many different
404 classes including some that have never before been seen in bacteria. This is in strong contrast to only
405 one or two DUBs encoded by most other intracellular bacteria. Interestingly, some of the *Simkania*
406 DUBs show cleavage specificity–SnOTU specifically cleaves linear M1 chains and VTD-type DUB
407 preferably cleaves K6-linked ubiquitin conjugates–while others are less specific (Boll *et al.*, 2023).
408 These observations indicate that Sne encodes ubiquitin-modifying enzymes to manipulate and
409 counteract the ubiquitin system of the host cell, but so far no Sne ubiquitin ligases have been
410 described.

411 Bioinformatical analysis revealed several genes in Sne that contain a RING domain. In the case of
412 SneRING, the RING as well as the C-terminal domain is shared with related proteins from other
413 *Chlamydia*-like bacteria. Despite the overall similarity, there are notable differences in the Zn-binding
414 residues of the RING finger, when comparing and aligning the sequences of the SneRING with the E3s
415 from the *Chlamydia*-like bacteria. In addition to these putative E3s of related bacteria, also two
416 established human RING fingers, structurally corresponding best to the SneRING model, were
417 included in the alignment. In particular, PDB:3LRQ_A (from TRIM37) structurally matches best;
418 however, it is more similar to the RING finger of the *Chlamydia*-like bacteria than of Sne in terms of
419 Zn binding (Fig 1). In addition to SneRING, Sne possesses several more proteins with a RING domain
420 (Fig S1), which remain to be characterized.

421 Though the RING finger of the SneRING appears to be rather atypical, we could demonstrate the
422 ligase activity using autoubiquitination assays. SneRING does not unspecifically interact with E2
423 enzymes, because we detected the activity of the SneRING only in the presence of the E2 conjugating
424 enzyme UbcH5b, and, to a lesser extent, in combination with the E2 UBE2T (Fig 2). However, the
425 human genome encodes for around 40 E2 conjugating enzymes that are involved in transferring
426 ubiquitin or ubiquitin-like proteins to the target (Stewart *et al*, 2016). We have tested only a limited
427 number of E2 enzymes, so we cannot exclude that SneRING is active in the presence of other E2
428 enzymes besides UbcH5b and UBE2T.

429 UbcH5b plays an important role in various cellular processes, such as in the activation of NF-κB by the
430 degradation of $I_{\kappa}b\alpha$ (Gonen *et al*, 1999) and regulation of the level of p53 by ubiquitination and its
431 subsequent degradation (Saville *et al*, 2004). It is involved in the removal of abnormal and regulatory
432 proteins (Seufert & Jentsch, 1990) and is one of the most active E2 enzymes (Houben *et al*, 2004). In
433 contrast, the E2 conjugating enzyme UBE2T regulates the levels of the receptor for activated protein
434 kinase C (RACK1) by mediating its ubiquitination with K48-linked conjugates followed by its
435 elimination. In this way, UBE2T induces hyperactivation of the Wnt/β-catenin signaling pathway (Yu *et*
436 *al*, 2021). The Wnt/β-catenin signaling pathway is crucial in various physiological processes ranging
437 from embryonic development to tissue homeostasis in adults (Liu *et al*, 2022). It is conceivable that
438 SneRING interacts with these E2 ligases during infection, considering their ubiquitous presence in the
439 cell. 3D structure prediction has helped identify S19 and E22 as crucial for the interaction with
440 UbcH5b, which was confirmed by an *in vitro* autoubiquitination assay (Fig 1C and Fig 2B). This shows
441 that the predicted RING domain of the SneRING is the interacting region with the E2 conjugating
442 enzyme UbcH5b. The expression of the catalytically inactive form of SneRING, however, did not
443 influence infection.

444 SneRING produces K6-, K11-, K48- and K63-linked ubiquitin conjugates, which implies that its host cell
445 targets are modified similarly (Fig 3 and Fig S2). The preference to catalyze K6 and K48 linkages was
446 also observed for the HECT-like ubiquitin ligase NleL of *Escherichia coli* O157:H7. (Lin *et al*, 2011). This
447 strain from the group of enterohemorrhagic *E. coli* (EHEC) causes hemorrhagic colitis and diarrhea in
448 humans (Lim *et al*, 2010). The bacterial infection is stimulated by the bacterial HECT-like ligase NleL,
449 which mediates the ubiquitination and inactivation of the host c-Jun NH2-terminal kinases (JNKs),
450 promoting the production of unique attaching and effacing (A/E) lesions (Sheng *et al*, 2017) and thus
451 a close adherence between the bacterium and the membrane of the epithelial cell (Nataro & Kaper,
452 1998). NleL shows *in vitro* ubiquitinating activity when incubated with the E2 conjugating enzyme
453 UbcH5b (Lin *et al.*, 2011), similar to SneRING.

454 Although not obligate intracellular, *Salmonella enterica* subsp. *enterica* serotype Typhimurium
455 replicates within a bacteria-containing vacuole after invading the host cell (Steele-Mortimer, 2008),
456 similar to Sne. SopA effector of *S.* Typhimurium is a HECT-like E3 ubiquitin ligase and preferentially
457 reacts with the host E2 ubiquitin-conjugating enzymes UbcH5a, UbcH5c, and UbcH7. It has been
458 proposed that SopA ubiquitinates bacterial and host cell proteins involved in *Salmonella*-induced
459 intestinal inflammation (Zhang *et al*, 2006). The ligase selectively mediates K11- and K48-linked
460 polyubiquitination of the human RING-ligases TRIM56 and TRIM65, leading to their proteasomal
461 degradation during infection. Blocking these ligases suppresses the expression of the nucleic acid-
462 sensing receptor STING and interferon-γ (Fiskin *et al*, 2017; Tripathi-Giesgen *et al.*, 2021). *S.*

463 Typhimurium virulence factor SspH2 has been shown to autoubiquitinate *in vitro* when combined
464 with the E2 enzyme UbcH5b and is thus assumed to be an E3 ubiquitin ligase, too, similar to HECT
465 type E3 ligases (Quezada *et al*, 2009). *In vitro* experiments revealed that SspH2 mediates K48-linked
466 ubiquitination, suggesting that it targets proteins for degradation by the proteasome (Levin *et al*,
467 2010). A putative homolog of SspH2, IpaH3 from *Shigella*, also mediates the synthesis of K48-linked
468 ubiquitin chains and it only shows activity in the presence of E2 conjugating enzymes of the UbcH5
469 type (Zhu *et al*, 2008). Ultimately, all the observations made in this study and parallels with known E3
470 ligases of other bacteria support the identification of SneRING as an E3 ubiquitin ligase with a role in
471 infection. Since genetic modification of Sne has so far not been achieved, we are currently unable to
472 confirm to which extent bacterial infectivity and life cycle depend on the activity of SneRING.

473 The variety of Sne DUBs, with 12 identified candidates of which 8 are active, indicates that ubiquitin-
474 modifying enzymes are important for Sne infection. As with other intracellular bacteria, Sne
475 replication niche SnCV can be a direct target for ubiquitination. This could lead to its complete or
476 partial degradation by autophagy (Hermanns & Hofmann, 2019). Sne DUBs might play an important
477 role in preventing autophagy by removing ubiquitin from the SnCV surface. The role of SneRING, on
478 the other hand, can be to modulate protein stability or activity through ubiquitination. While some
479 Sne DUBs do not show cleavage specificity, others are only active against certain ubiquitin chain
480 types. Interestingly, the two Sne-encoded DUBs SnJos1 and SnJos2 efficiently cleave K6-, K11-, K48-
481 and K63-linked ubiquitin chains, with another enzyme selectively cleaving K6-linked chains (Boll *et al.*,
482 2023). One possibility is that SneRING generates these specific ubiquitin conjugates in the early
483 stages of infection for them to be removed at later stages by Sne DUBs to support bacterial
484 development and/or release. However, whether the targets of both SneRING and Sne DUBs are
485 bacterial or host cell proteins remains yet to be determined.

486 SnCV has a unique tubular morphology and is in close contact with ER. Its development depends on
487 retrograde vesicular transport (Herweg *et al.*, 2016) and it is presumed that the majority of lipids for
488 growth of this complex membranous compartment are derived from ER. Sne is also capable of
489 suppressing ER stress response (Mehlitz *et al.*, 2014). On the other hand, mitochondria intertwine
490 with SnCV only in the early stages of infection, whereas at the later time point, we observe
491 fragmentation and loss of mitochondrial mass. Endogenous SneRING is found in the ER/SnCV
492 membrane (Herweg *et al.*, 2016), whereas the overexpressed SneRING localizes to cytosol, ER, and
493 mitochondria (Fig 4 and Fig S4), including its surprising association with the inner mitochondrial
494 membrane (Fig 4D). This, together with the identification of possible targets and interacting factors,
495 might offer a clue about the function of this enzyme.

496 Mitochondrial depolarization leads to the formation of K6-, K11-, K48-, and K63-chain linkages on the
497 surface of these organelles. Parkin, a mitochondrial protein with E3 ubiquitin ligase activity and the
498 potential to form these same linkages is involved in mitochondrial ubiquitination, which promotes
499 mitophagy (Harper *et al*, 2018). Recently, Parkin has been shown to ubiquitinate proteins not only on
500 the surface of mitochondria but also in the inner membrane. Parkin directly binds to prohibitin 2
501 (PHB2) through its RING1 domain and promotes K11- and K33-linked ubiquitination of PHB2 (Sun *et*
502 *al*, 2022), which enhances the interaction between PHB2 and the central protein in autophagy, LC3
503 (Wei *et al*, 2017). SneRING not only generates the same types of ubiquitin chains in an *in vitro*
504 reaction as Parkin (Fig. 3), but one of the highly enriched host cell proteins in the SneRING pulldown
505 fractions is PHB2 (Fig 5, Table S1). SneRING might ubiquitinate PHB2 to induce mitophagy; however,
506 this process would depend on the presence of SnCV and other, so far unidentified bacterial factors,
507 since we did not observe mitochondrial fragmentation in non-infected cells expressing SneRING (Fig
508 S4). Alternatively, SneRING/prohibitin interaction might impact mitochondrial integrity and
509 respiration, in which prohibitins play an important role (Merkwirth & Langer, 2009). This could also
510 explain another highly enriched putative SneRING interactor, BCAP31, a protein present in ER-
511 mitochondria contact sites, which has been reported to regulate mitochondrial respiration by
512 controlling the mitochondrial import of respiratory complex I subunits (Namba, 2019). Interestingly,
513 ERLIN1 and ERLIN2, other highly enriched hits (Fig 5, Table S1), also contain a prohibitin domain.
514 These proteins localize to ER and are involved in ERAD (Pearce *et al.*, 2009), which might be a
515 potential target of modification by SneRING considering that bacteria can suppress ER stress response
516 (Mehlitz *et al.*, 2014), a process counteracted by the ERAD upregulation (Hwang & Qi, 2018). Finally,
517 possible SneRING ubiquitination of CKAP4, a protein involved in the attachment of ER to microtubules
518 (Vedrenne *et al*, 2005), might be required during the growth and organization of the SnCV. CKAP4 has
519 recently been reported to also play a role in ER-phagy, a process triggered by ER stressors, such as
520 tunicamycin (Li *et al*, 2024). Its targeting by SneRING might be one of the ways for bacteria to
521 interfere with ER stress signaling (Mehlitz *et al.*, 2014). Though interesting, these theories must be
522 confirmed by analyzing if any of these proteins are ubiquitinated upon SneRING expression or during
523 infection. In addition, deletion of SneRING from bacteria could give further information about the
524 function and importance of this protein.

525 To survive and replicate within their host, intracellular pathogens have evolved various strategies and
526 mechanisms to counteract the host cell immune system. By secreting effector proteins, pathogens
527 manipulate the host cell to provide better conditions for their survival and propagation. Effector
528 proteins also include ubiquitin-modifying enzymes such as deubiquitinases and ubiquitin E3 ligases.
529 This study describes for the first time a Sne effector protein SneRING that functions as ubiquitin E3
530 ligase with a possible role in remodeling host cell mitochondria and ER and controlling mitophagy and

531 ER stress response to promote the development of SnCV and accommodate its unique replicative
532 niche.

533

534 Materials and Methods

535 Sequence analysis

536 Sequence alignments were generated using the MAFFT package (Katoh & Standley, 2013).
537 Generalized profiles were derived from multiple alignments using pftools (Bucher *et al.*, 1996) and
538 searched against the Uniprot database (https://www.uniprot.org) and the NCBI microbial genome
539 reference sequence database (https://www.ncbi.nlm.nih.gov/genome/microbes) using pfsearchV3
540 (Schuepbach *et al*, 2013). Structure predictions were run using a local installation of Alphafold 2.3
541 (Jumper *et al.*, 2021). Structure comparisons were performed using the DALI software (Holm, 2022).
542 For modeling the missing Zn^{2+} ions into Alphafold structures, a superposition with the best-scoring
543 Zn^{2+}-containing DALI hit was used to copy the zinc ions into the model. Subsequently, an energy
544 minimization was performed using YASARA (Krieger & Vriend, 2014) to improve the sidechain
545 positioning of the Zn^{2+} ligands.

546 Cloning and mutagenesis

547 The SneRING coding region for protein purification was obtained by amplification of *S. negevensis*
548 genomic DNA (Leibniz Institute DSMZ, German Collection of Microorganisms and Cell Cultures, DSM
549 No. 27360) using the following primers: forward, 5'-
550 AAGTTCTGTTTCAGGGCCCGGAAAGGGTAAATCCTAATCAAGTTCTA – 3', and reverse, 5'-
551 ATGGTCTAGAAAGCTTTATGAAAAAATTCTACGAGAAATATCTTCC – 3'. Amplification was performed using
552 the Phusion™ High Fidelity DNA Polymerase Kit (Thermo Fisher Scientific, Massachusetts, USA), and
553 the PCR product was inserted into the pOPIN-K vector (Berrow *et al*, 2007) by restriction cloning
554 according to the manufacturer's protocol. Point mutations were generated using the QuikChange
555 Lightning kit (Agilent Technologies, California, USA). To introduce the first mutation, the following
556 primers were used: forward, 5' – GCATGGAATTGTCGCAGGTGCTGGGAACCAATTCA – 3', and reverse, 5'
557 – TGAATTGGTTCCCAGCACCTGCGACAATTCCATGC – 3'. The second mutation was added by using the
558 following primers: forward, 5' – AATTGTCGCAGGTGCTGGAGACCAATTCAGGATGGTCC – 3', and reverse,
559 5' – GGACCATCCTGAATTGGTCTCCAGCACCTGCGACAATT – 3'. SneRING coding region for transfection
560 experiments was synthesized by Thermo GeneArt Gene synthesis (Thermo Fisher Scientific,
561 Massachusetts, USA) and cloned into the pCDNA3 vector by restriction digestion according to the
562 manufacturer's protocol.

563 Protein expression and purification

564 Wildtype SneRING was expressed from the pOPIN-K vector containing an N-terminal 6His-GST-tag in
565 *E. coli* Rosetta (DE3) pLysS. The bacteria culture was grown in LB medium at 37 °C until reaching an
566 OD_{600} of 0.8. Afterward, the culture was precooled at 18 °C before SneRING expression was induced
567 with 500 µM $ZnCl_2$ and 0.1 mM isopropyl β-d-1-thiogalactopyranoside (IPTG) for 16 h when bacteria
568 were collected by centrifugation at 5,000 x g for 15 min. The pellets were frozen at -80 °C, then
569 thawed on ice and resuspended in binding buffer (300 mM NaCl, 20 mM Tris pH 7.5, 20 mM
570 imidazole, 2 mM β-mercaptoethanol), containing DNase and lysozyme. Cells were sonicated for 10
571 min with 10 s pulses at 50 W and the lysate was clarified by centrifugation for 1 h at 50,000 x g and 4
572 °C. The supernatant was applied to a HisTrap FF column (Cytiva, Massachusetts, USA), and affinity
573 purification was performed according to the manufacturer´s protocol. The subsequent incubation of
574 the fractions with 3C protease during dialysis in binding buffer overnight resulted in the 6His-GST tag
575 removal, which was removed, together with the His-tagged 3C protease in a second affinity
576 purification run. Size exclusion chromatography (HiLoad 16/600 Superdex 75 pg (Cytiva,
577 Massachusetts, USA)) was performed in a buffer containing 20 mM Tris pH 7.5, 150 mM NaCl, and 2
578 mM dithiothreitol (DTT). After concentration using VIVASPIN 20 Columns (Sartorius, Göttingen,
579 Germany), the purified protein was frozen in liquid nitrogen and stored at -80 °C.

580 The expression of SneRING S19R_E22R was induced as already described for the wildtype SneRING.
581 After harvesting the cells, the pellet was resuspended in lysis buffer (40 mM Tris pH 8.2, 500 mM
582 NaCl, 10 mM β-mercaptoethanol, 10 mM imidazole, containing 1xComplete™ protease inhibitor
583 cocktail (Roche Holding, Basel, Switzerland), DNase and lysozyme). Cells were lysed by sonication,
584 the cleared lysate was applied to Ni-NTA agarose (Qiagen, Hilden Germany), and affinity purification
585 was performed according to the manufacturer´s protocol. Mutated SneRING was eluted using 40 mM
586 Tris pH 7.5, 500 mM NaCl, 10 mM β-Mercaptoethanol, and 250 mM imidazole. The removal of the
587 6His-GST tag was performed similarly to the wildtype SneRING and using the Ni-NTA agarose (Qiagen,
588 Hilden Germany) in a buffer containing 20 mM Tris pH7.5 and 300 mM NaCl. After concentration on
589 Amicon Ultra-15, PLGC Ultracel-PL membrane (Sigma/Merck, Darmstadt, Germany), the protein was
590 frozen in liquid nitrogen and stored at -80 °C.

591 The two Sne DUBs SnVTD and SnOTU used in the study were purified as described before (Boll *et al.*,
592 2023). The plasmids pOPINB-OTUB1* (Addgene plasmid #65441; http://n2t.net/addgene:65441;
593 RRID:Addgene_65441), pOPINB-AMSH* (Addgene plasmid #66712; http://n2t.net/addgene:66712;
594 RRID:Addgene_66712) (Michel *et al*, 2015), pOPINK-Cezanne (OTU, aa 53-446), (Addgene plasmid
595 #61581; http://n2t.net/addgene:61581 ; RRID:Addgene_61581) (Mevissen *et al*, 2013) and pOPINS-
596 USP21 (USP, aa 196-565) (Addgene plasmid #61585; http://n2t.net/addgene:61585;
597 RRID:Addgene_61585) (Ye *et al.*, 2011) were kind gifts from David Komander (WEHI, Melbourne,
598 Australia). Purification of these DUBs was performed as already described for the SneRING.

599 Protein concentration was determined by measuring the absorption at 280 nm (A_{280}) and using the
600 SneRING extinction coefficient calculated from its sequence.

601 ***In vitro* autoubiquitination assay**

602 10 µL of the 10x ligation buffer (800 mM Tris pH 7.5, 200 mM $MgCl_2$, 12 mM DTT) was mixed with 10
603 µM purified recombinant SneRING, 100 nM recombinant E1 ubiquitin-activating enzyme and 2.3 µM
604 recombinant E2 ubiquitin-conjugating enzyme, to which 50 µM recombinant ubiquitin and 10 mM
605 ATP were added. ddH_2O was added to a final volume of 100 µL. The reactions were incubated at 37 °C
606 for different time points (0 min, 30 min, 60 min, 120 min, 180 min, and 300 min) and stopped by
607 adding Laemmli sample buffer (62.5 mM Tris pH 6.8, 2% SDS, 10% glycerol, 5% β-mercaptoethanol,
608 and 0.002% Bromophenol Blue) and analyzed by sodium dodecyl sulfate-polyacrylamide gel
609 electrophoresis (SDS-PAGE) and western blot.

610 The purified proteins of the E2 conjugating enzymes UbcH5b, UbE2T, UbCH7, Ube2A, Ube2B and
611 Ube2W were a kind gift from David Komander (WEHI, Melbourne, Australia).

612 **UbiCRest assay**

613 The recombinant DUBs were first diluted in a buffer containing 150 mM NaCl, 20 mM Tris pH 7.5, and
614 10 mM DTT. The 5 h *in vitro* autoubiquitination assay reaction was treated for 15 min at RT with 2 mU
615 apyrase to remove the remaining ATP. For the assay, the DUBs were added at 1.5 µM concentration
616 except OTUB1, for which 3 µM concentration was used. During the double UbiCrest assay, the DUBs
617 were added at 1.5 µM or 0.75 µM concentrations. The mixture was incubated for 1 h at RT and the
618 reaction was stopped by adding Laemmli sample.

619 **Immunoblotting**

620 The lysates for western blot analysis were prepared with Laemmli sample buffer and denatured at 95
621 °C for 5 min. After SDS-PAGE, proteins were transferred onto a PVDF membrane. The membrane was
622 blocked with 5% milk in Tris-based saline (TBS) and incubated in the primary antibody, followed by
623 the incubation with an HRP-coupled secondary antibody (1:3000) in a blocking solution. The signal
624 was detected using SuperSignal™ West Femto Maximum Sensitivity Substrate (Thermo Fisher
625 Scientific, Massachusetts, USA) and a Chemo Cam Imager (Intas). In the case of an affimer, the
626 membrane was incubated overnight at 4 °C in the affimer dilution in TBS. The next day, the
627 membrane was washed with TBS and incubated with a 6xHis primary antibody, followed by the HRP-
628 coupled secondary antibody as already described.

629 **Cell culture**

630 HeLa (ATCC® CCL-2.1™), HeLa229 KDEL-dsRed, Hela 229 Mito-GFP, and THP-1 (ATCC® TIB-202™) cells
631 were grown in Roswell Park Memorial Institute (RPMI)1640 medium (Thermo Fisher Scientific,
632 Massachusetts, USA), Hek293T cells (ATCC® CRL-3216™) were grown in Dulbecco's modified Eagle's
633 medium (DMEM) medium (Thermo Fisher Scientific, Massachusetts, USA) and U2OS cells (ATCC®
634 HTB-9.6™) were grown in DMEM/F12 medium (Thermo Fisher Scientific, Massachusetts, USA). All
635 media were supplemented with 10% v/v heat-inactivated (56 °C at 30 min) fetal calf serum (FCS)
636 (Sigma/Merck, Darmstadt, Germany). Growth took place at 37 °C and 5% CO_2. To differentiate THP-1
637 cells into macrophages, 5x 10^5 cells/well were seeded into 6-well plates and incubated with 20 ng/mL
638 phorbol 12-myristate 13-acetate (PMA) (Sigma/Merck, Darmstadt, Germany) in RPMI1640 medium
639 containing 10% v/v heat-inactivated FCS for 24 h. The medium was exchanged for fresh RPMI1640
640 medium containing 10% v/v heat-inactivated FCS and the cells were incubated for a further 48 h.

641 Primary human macrophages were derived from peripheral blood mononuclear cells (PBMCs)
642 isolated from leukoreduction system (LRS) cones, using the SepMate™-50 system (#85450, STEMCELL
643 Technologies, Cologne, Germany) and Ficoll-Paque (#GE17-1440-03, Sigma/Merck, Darmstadt,
644 Germany) gradient according to manufacturer's instructions. Red blood cells were removed by hypo-
645 osmotic shock: PBMC pellets were mixed and incubated with 16 mL sterile water for 30 s, then
646 immediately 4 mL 5 x DPBS were added. Monocytes were purified from the PBMC fraction using the
647 EasySep™ Human CD14 Positive Selection Kit II (# 17858, STEMCELL Technologies, Cologne, Germany)
648 according to the manufacturer's instructions and seeded in 6-well cell culture plates (1.5 x 106
649 cells/well) in medium supplemented with 50 ng/mL M-CSF (#78057, STEMCELL Technologies,
650 Cologne, Germany). Medium exchanges, with fresh M-CSF supplementation, were done on days 1
651 and 4. On day 7, M2"-like polarization, was induced by replacing M-CSF-containing medium with
652 medium containing 100 ng/mL IL-4 (#78045, STEMCELL Technologies, Cologne, Germany) and further
653 incubation for 48 h. All cultivation steps were done in RPMI1640 (Thermo Fisher Scientific,
654 Massachusetts, USA) supplemented with 10% (v/v) heat-inactivated FCS (Sigma/Merck Darmstadt,
655 Germany). All Sne infection experiments were performed on day 9, without cytokine
656 supplementation.

657 *Acanthamoeba castellanii* (ATCC® 30010D™) were cultured in axenic medium (56 mM glucose, 2.6
658 mM KH2PO4, 1.3 mM Na2HPO4x7H2O, 0.5% proteose peptone 2, 0.5% thiotone E peptone, 0.5%
659 yeast extract) in cell culture flasks at 30 °C.

660 **Bacteria and infection**

661 *E. coli* DH5α and Rosetta (DE3) pLysS were grown in an LB medium containing the respective
662 antibiotics for selection (1% bacto-tryptone, 0.5% yeast extract, 1% NaCl, 1% agar).

663 To prepare *S. negevensis* (ATCC® VR-1471™), U2OS cells were grown to 60% confluency, and infected
664 at a multiplicity of infection (MOI) 1 in RPMI1640 medium without HEPES containing 5% v/v heat-
665 inactivated FCS (infection medium). The infected cells were incubated at 35 °C and 5% CO_2 for 6 h,
666 when the medium was exchanged for fresh infection medium. After 3 days of growth under the same
667 conditions, the cells were detached using a cell scrapper and lysed by vortexing the cells with 2-5 mm
668 glass beads (Carl Roth, Karlsruhe, Germany). Intact cells and larger cell debris were removed by low-
669 speed centrifugation at 600 x g for 10 min and the resulting supernatant was centrifuged at 20,000 x
670 g for 30 min to pellet the released bacteria. The pellet was resuspended in 5 mL SPG buffer (250 mM
671 sucrose, 4 mM monopotassium phosphate, 10 mM disodium phosphate, and 5 mM glutamate pH
672 7.4), followed by centrifugation (20,000 x g, 30 min), with the resulting pellet resuspended in 2.5 mL
673 SPG buffer. The bacteria were homogenized using a syringe with one G20 and one G18 needle,
674 aliquoted, and stored at -80 °C. All the experiments with *S. negevensis* were performed in a
675 laboratory with biosafety level 2, which is registered with the Lower Franconia Government under
676 code 55.1-8791.1.30.

677 For infection experiments, 5 x 10^5 human cells/well were seeded into 6 well plates and at 60%
678 confluency infected with *S. negevensis* at MOI 1 in the infection medium, at 35 °C and 5% CO_2. 6 h
679 later, the medium was exchanged for fresh infection medium. The infection proceeded for the
680 indicated time points. When infection took longer than 3 days, the medium was exchanged for fresh
681 infection medium after every 3 days.

682 *A. castellanii* were seeded into cell culture flasks and infected with *S. negevensis* in an axenic
683 medium. Infected amoebae were incubated at 30 °C for 4 days.

684 **Transfection**

685 Hek293T cells were transfected using the Calcium-phosphate transfection method as described
686 previously (Wagner *et al*, 2019). For 6-well plates, 4 µg of the respective plasmid were used; for
687 transfecting cells in 15 cm dishes, we used 50 µg of plasmid DNA. U2OS and HeLa229 cells were
688 transfected using the commercially available transfection reagents jetOptimus® (Polyplus®, Illkirch-
689 Graffenstaden, France) or PEI MAX® (Polysciences, Inc., Warrington, United Kingdom) according to
690 the manufacturer's protocol. Depending on the experiment, cells were infected with *S. negevensis* at
691 MOI 1, 24 h post-transfection.

692 **Immunofluorescence and Microscopy**

693 U2OS and HeLa cell lines were seeded at a density of 8 x 10^4 cells/well into 12 well plates, while
694 Hek293T cells were seeded at a density of 5 x 10^5 cells/well into 6 well plates on 15 mm glass
695 coverslips (Paul Marienfeld, Lauda-Königshofen, Germany). Cells were transfected and/or infected as

696 indicated in the corresponding experiments. The cells were fixed at respective time points using 4%
697 paraformaldehyde (PFA) in PBS for 1 h at RT. For *S. negevensis* infection experiments, the cells were
698 permeabilized with 0.2% Triton X-100 in PBS for 45 min at RT while shaking, washed with PBS, and
699 blocked in 2% goat serum in PBS for 1 h, followed by staining with a SnGroEL primary antibody in the
700 blocking solution overnight at 4 °C. The following day, samples were washed and incubated with the
701 secondary antibody (1:1600) and DAPI (1:3000) for 1 h in 2% goat serum in PBS at RT. After washing
702 with PBS and ddH_2O, coverslips were mounted using Mowiol 4-88 (Carl Roth GmbH + Co. KG,
703 Karlsruhe, Germany).

704 For experiments that did not include infection, after fixing, cells were simultaneously permeabilized
705 and blocked for 30 min at RT in blocking solution (10% BSA, 0.2% Triton X-100, in PBS), washed with
706 PBS and stained with the primary antibody diluted in antibody dilution solution (3% BSA in 0.05%
707 Tween in PBS) for 1 h at RT. After washing with PBS and blocking for 10 min in blocking buffer at RT,
708 samples were washed again and incubated with DAPI (1:3000) and the secondary antibodies (1:100)
709 for 1 h at RT. The coverslips were then washed with PBS and ddH_2O and mounted using Mowiol 4-88
710 (Carl Roth GmbH + Co. KG, Karlsruhe, Germany). Microscopy was performed using LEICA SP5 confocal
711 laser scanning microscope.

712 **RNA isolation, cDNA synthesis, and RT-qPCR**

713 Infected macrophages were collected on day 2, 4 and 6 pi. The cells were washed with DPBS at the
714 desired time point and 100 µL of fresh medium and 500 µL RNAprotect Cell Reagent (Qiagen, Hilden,
715 Germany) were added per well. Detached cells were collected in RNase-free tubes and stored at 4 °C
716 for a maximum of 1 week. After centrifugation at 6200 x g for 5 min at 4 °C, 600 µL RLT Buffer
717 supplemented with β-mercaptoethanol was added to each pelleted sample, and RNA was purified
718 using the RNeasy Mini kit (Qiagen, Hilden, Germany) according to manufacturer's instructions. For
719 other human cell lines, after collecting them on day 2 and 4 pi and washing with DPBS at the desired
720 time point, 600 µL RLT Buffer supplemented with β-mercaptoethanol was added to each sample and
721 RNA was purified using the RNeasy Mini (Qiagen, Hilden, Germany) according to manufacturer's
722 instructions. DNase treatment was performed using the TURBO DNA-free™ Kit (Invitrogen, California,
723 USA). 100 ng pure RNA was used for cDNA generation, using the Revert Aid First Strand cDNA
724 Synthesis Kit (Thermo Fisher Scientific, Massachusetts, USA). RT-qPCR was performed on a
725 StepOnePlus™ instrument (Life Technologies, California, USA), using the GreenMasterMix (2X) High
726 ROX™ (Gennaxon, Ulm, Germany). Data analysis was performed using the StepOne Software (v2.3)
727 and Microsoft Excel, with a modified $2^{-\Delta\Delta Ct}$) method (Livak & Schmittgen, 2001). ΔCt values were
728 calculated relative to the host reference gene *YWHAZ* (human) or the 5S RNA (for amoeba). Fold
729 changes ($2^{-\Delta\Delta Ct}$) of gene expression for each tested Sne gene, were calculated relative to the non-

730 infected controls. The following primers were used: forward, 5' – ATACTGCGCAGAAAGCAC – 3', and
731 reverse, 5' – ACCCCAGTACTAACACCG – 3' (5S RNA reference gene for amoeba); forward, 5' –
732 GCAGAGTCGAAGTTTCAAGGG – 3', and reverse, 5' – TCGCTTGCCTGTTGAGGATT – 3' (SneRING);
733 forward, 5' – TTCCATCACCGGCAACATCA – 3', and reverse, 5' – GCAAAAGAGATCGCGCTGAA – 3' (GroEL
734 C (SNE_A22590)); forward, 5' – CACCTGATCCCATCCCGAAC – 3', and reverse, 5' –
735 GCGACCTACTCTCCCGTACT – 3' (Sne 5S RNA) (Boll *et al.*, 2023); forward, 5' –
736 ACTTTTGGTACATTGTGGCTTCAA – 3', and reverse, 5' – CCGCCAGGACAAACCAGTAT – 3'(*YWHAZ*)
737 (Vandesompele *et al*, 2002).

738 **Mitochondrial isolation and fractionation**

739 Mitochondria were isolated from cells transfected for 48 h as described previously (Humphries *et al*,
740 2005). Cellular fractionation and determining of submitochondrial localization by swelling and PK
741 treatment were performed as already described (Kozjak-Pavlovic *et al*, 2011; Kozjak *et al*, 2003).
742 Carbonate extraction for determining protein membrane extractability was performed as previously
743 described (Milenkovic *et al*, 2004). In brief, isolated mitochondria from transfected cells were either
744 sonicated in 10 mM Tris pH 7.6 and 500 mM NaCl or treated with 100 mM Na_2CO_3 at pH 10.8 or 11.5
745 for 20 min on ice. After centrifugation at 100.000 g, pellets were resuspended in Laemmli sample
746 buffer, while supernatant and non-centrifuged control samples were precipitated using
747 trichloroacetic acid (TCA).

748 **Antibodies, chemicals, and positive controls**

749 K48- and K63-linked ubiquitin chains were components of the Di-ubiquitin Explorer Panel purchased
750 from UbiQ (Amsterdam, Netherlands, Cat. No. UbiQ-L01). M1-linked ubiquitin chains (kindly provided
751 by S. Meyer and A. Buchberger) were produced by incubating the following reaction mixture at 37 °C
752 for two hours: 6 µg bovine ubiquitin, 200 ng yeast Uba1, 600 ng human UbcH5c, 4 µg HOIP RBR-LDD
753 (Smit *et al*, 2012) in a buffer containing 50 µL 20 mM Tris/HCl pH 7.5, 5 mM $MgCl_2$, 1 mM DTT, 4 mM
754 ATP.

755 The primary antibodies against ubiquitin (Cat. No. 05-9449), FLAG-tag (Cat. No. F7425), CPOX (Cat.
756 No. HPA015736), K63-linked ubiquitin chains (Cat. No. 05-1308), K48-linked ubiquitin chains (Cat. No.
757 05-1307) and M1-linked ubiquitin chains (Cat. No. MABS451, kindly provided by A. Buchberger) were
758 purchased from Sigma/Merck (Darmstadt, Germany). The anti-ubiquitin Lys6 specific Affimer® (Cat.
759 No. MABS1918, kindly provided by M. Eilers) was purchased from Sigma/Merck (Darmstadt,
760 Germany). The primary antibodies against Tubulin (Cat. No. ab18251) and Mitofilin (Cat. No.
761 ab48139) were purchased from Abcam (Cambridge, United Kingdom). The primary antibodies against
762 Calnexin (Cat. No. 2433, Cat. No. sc-23954) were purchased from Cell Signaling (Massachusetts, USA)

763 and Santa Cruz Biotechnology (Texas, USA). The antibody against GAPDH (Cat. No. sc-47724) was
764 purchased from Santa Cruz Biotechnology (Texas, USA). The anti-HSP60 antibody (Cat. No. ADI-SPA-
765 806) was purchased from Enzo Life Sciences (New York, USA). The primary antibody against TIM44
766 (Cat. No. 612582) was purchased from BD Transduction Laboratories (California, USA). The antibody
767 against 6xHis (Cat. No. GTX18184) was purchased from Biozol (Eching, Germany). The antibody
768 against K11-linked ubiquitin chains (Cat. No. NBP3-05681, kindly provided by A. Buchberger,) was
769 purchased from Novus Biologicals (Littleton, USA). The antibody against Sam50 was custom-
770 generated against the full-length protein (Gramsch laboratories, Schwabhausen, Germany). The
771 antibody against rat Tom70 (crossreactive with human Tom70) was a gift from K. Mihara. The
772 antibody against SnGroEL was produced as described in a previous study (Mehlitz *et al.*, 2014).
773 Secondary antibodies anti-rabbit-Alexa555, Cat. No. A-21428, anti-mouse-Alexa488 Cat. No. A-11001,
774 and anti-mouse-Alexa555, Cat. No. A-21422 were purchased from Thermo Fisher Scientific
775 (Massachusetts, USA). Anti-rabbit-Atto647N secondary antibody, Cat No. 40839, was purchased from
776 Sigma/Merck (Darmstadt, Germany). Anti-mouse-Cy2 secondary antibody, Cat. No. 115-225-146, as
777 well as the HRP-coupled secondary antibodies for western blot, were purchased from Biozol (Eching,
778 Germany).

779 **Immunoprecipitation**

780 For immunoprecipitation (IP) assays, U2OS cells were seeded at a density of 1.2 x 10^6 cells/well into
781 10 cm dishes. The next day, the cells were transiently transfected with a plasmid carrying a FLAG-
782 tagged humanized version of the SneRING gene and 24 h later infected with Sne at an MOI 1. Non-
783 transfected and non-infected cells served as controls. On day 2 pi, the cells were washed once with
784 PBS, harvested in lysis buffer (20 mM Tris pH 7.5, 150 mM NaCl, 0.1 % NP-40, proteinase inhibitor
785 (Roche: cOmplet, EDTA-free Protease Inhibitor Cocktail), 1 mM PMSF, 5 mM Iodoacetamide)),
786 incubated for 30 min at 4 °C and sonicated for 15 min using an ultrasonic water bath. After removing
787 the cell debris by centrifugation (15 min, 14000 x g, 4 °C), the supernatant was added to equilibrated
788 Anti-FLAG® M2 magnetic beads (Sigma/Merck, Darmstadt, Germany) and incubated on a rotary
789 shaker overnight at 4 °C. The beads were washed three times for 5 min at 4 °C with washing buffer
790 (20 mM Tris pH 7.5, 150 mM NaCl, 0.1% NP-40) and once with a buffer containing 20 mM Tris pH 7.5,
791 150 mM NaCl. For mass spectrometry analysis, bound proteins were eluted with 200 µg/mL FLAG
792 peptide (Sigma/Merck, Darmstadt, Germany) in elution buffer (6 M urea, 2 M thiourea).

793 **Mass spectrometry analysis**

794 For in-solution digest, the samples were reduced by adding 1 µL of 1 M DTT for 1 h at RT, alkylated
795 with 1 µL of 400 mM chloroacetamide (CAA) for 45 min at RT in darkness, digested with 1 µL of the
796 Lysyl endopeptidase (Lys-C, 0.5 µg/µL) for 3 h at RT, treated with 270 µL of 50 mM triethylammonium

797 bicarbonate buffer and finally digested with 1 µL of trypsin enzyme (1 µg/µL) overnight at RT. The
798 next day, samples were acidified by adding 1 µL of 100% formic acid. After in-solution digestion,
799 peptides were bound to styrene-divinylbenzene reverse-phase stage tips (SDB-RP). One stage tip was
800 used per sample. The stage tips were equilibrated by adding 20 µL of 100% methanol and
801 centrifuging for 1 min at 700 x g. Afterward, 20 µL of buffer B (0.1% formic acid in 80% acetonitrile)
802 was added and the stage tips were again centrifuged for 1 min at 700 x g. In the next step, 20 µL of
803 buffer A (0.1 % formic acid in water) was added to each stage tip, the samples were centrifuged for 1
804 min at 700 x g and an additional 20 µL of buffer A was added. Acidified samples were spun down for 5
805 min at 17,000 x g, the supernatant was loaded onto the SDB discs of the equilibrated stage tips, and
806 they were again centrifuged for 5 min at 700 x g. The stage tips were washed buffers A and B and
807 completely dried with a syringe.

808 After binding peptides to SDB-RP Stage tips, they were analyzed by liquid chromatography-mass
809 spectrometry/mass spectrometry (LC-MS/MS). LC-MS/MS analysis was performed by the Proteomics
810 Facility of the CECAD, University of Cologne, as described previously (Hermanns *et al*, 2018).

811

812 Figure legends

813 **Figure 1. SneRING is a predicted RING domain ligase. (A)** Multiple alignment of the RING domains of
814 SneRING (Sne_A12920), some bacterial relatives (Sim-KFB93: *Simkaniaceae* bacterium
815 RefSeq:QVL56959; Sim-QNJ27: *Simkaniaceae* bacterium RefSeq:MDJ0651792; Chl-HKST: *Chlamydiia*
816 bacterium Uniprot: A0A960X5Q0), and sequences of the two best DALI hits (pdb:3LRQ (TRIM37 from
817 *Homo sapiens*) and pdb:2CKL (RING2 from *Mus musculus*)). Residues invariant or conserved in at least
818 50% of the sequences are shown on black and grey background, respectively. Residues involved in
819 the coordination of Zn_1 and Zn_2 are highlighted in red and magenta, respectively. **(B)** Alphafold model
820 of SneRING shows the N-terminal RING-like domain (blue) and a C-terminal domain of unknown
821 function (DUF, green). The Zn_1 and Zn_2 ions coordinated by the RING-like domain are shown in red
822 and magenta, respectively. **(C)** Alphafold model of the RING domain of SneRING (blue) in contact with
823 UbcH5b (grey). The Zn_1 and Zn_2 ions coordinated by the RING-like domain are shown in red and
824 magenta, respectively. The predicted contact residues Glu-22 (E22) and Ser-19 (S19) and their
825 interaction partners are labeled.

826 **Figure 2. SneRING shows ubiquitination activity in an *in vitro* assay. (A)** Purified recombinant
827 SneRING was mixed with recombinant E1 ubiquitin-activating enzyme, E2 ubiquitin-conjugating
828 enzyme (UbcH5b), ubiquitin, and ATP for indicated periods. A reaction without the ligase served as a
829 control. Samples were analyzed by SDS-PAGE and western blot, using an antibody against ubiquitin.

830 **(B)** *In vitro* autoubiquitination reaction of wildtype SneRING and SneRING-ligase with mutated E2
831 enzyme interacting region (SneRING S19R_E22R) was performed for 5 h as in A and analyzed by SDS-
832 PAGE and western blot, using anti-ubiquitin antibodies. **(C)** *In vitro* autoubiquitination reaction of
833 wildtype SneRING was performed as in A in combination with indicated E2 enzymes for 5 h, followed
834 by SDS-PAGE and western blot analysis using ubiquitin antibody. **(D)** SneRING was incubated with E2
835 enzyme UbcH5b or UBE2T in an *in vitro* autoubiquitination assay as described in A. Samples were
836 taken at indicated time points and tested by immunoblot using the primary antibody against
837 ubiquitin.

838 **Figure 3. SneRING generates K6-, K11-, K48, and K63-linked ubiquitin chains that can be digested by**
839 **specific DUBs. (A)** An *in vitro* autoubiquitination reaction as in Fig. 2A was incubated for 5 h, after
840 which an UbiCRest assay was performed using the indicated chain type-specific DUBs for 1 h at room
841 temperature. Ubiquitin chain cleavage was analyzed by SDS-PAGE and western blot using a primary
842 antibody against ubiquitin. **(B)** An *in vitro* autoubiquitination reaction as in A was incubated with
843 Cezanne (K11-linked ubiquitin chain-specific DUB) and AMSH (K63-linked ubiquitin chain-specific
844 DUB). Degradation of ubiquitin chains was detected by SDS-PAGE and western blot using anti-
845 ubiquitin antibody. **(C, D)** A 5 h *in vitro* autoubiquitination reaction of SneRING with UbcH5b (C) or
846 UBE2T (D) was analyzed by mass spectrometry. The graphs show $\log_{10}$ intensities of GlyGly-modified
847 residues for the different linkage types, as determined by MaxQuant.

848 **Figure 4. SneRING localizes to the host cell cytosolic, light membranes, and inner mitochondrial**
849 **membrane after overexpression. (A)** U2OS cells were transfected with a human codon-adjusted
850 FLAG-tagged version of the SneRING using the transfection reagent PEI MAX®. 72 h post-transfection,
851 cells were fixed and stained using DAPI (blue channel), and a primary antibody against FLAG followed
852 by the fluorophore-coupled secondary antibody (green channel). Images were taken using laser
853 scanning confocal microscopy. The scale bar represents 30 µm. **(B)** U2OS cells were transfected as in
854 A, and 36 h post-transfection, analyzed by SDS-PAGE and western blot using antibodies against the
855 FLAG-tag and tubulin. **(C)** U2OS cells were transfected as in A, and 48 h post-transfection, the cells
856 were separated by differential centrifugation into a crude mitochondrial (Mito), light membrane (LM),
857 and cytosolic (Cyt) fraction. Total cell lysate of non-transfected cells (Control) and transfected cells
858 (Total) served as control. The samples were analyzed by SDS-PAGE and western blot using antibodies
859 against Mic60, Calnexin, Tubulin, GAPDH, and FLAG. **(D)** U2OS cells were transfected as in D. After 48
860 h of expression, mitochondria were isolated and then incubated in isotonic buffer (-Swelling) or in
861 hypotonic buffer (+Swelling) to rupture the outer mitochondrial membrane, combined with the
862 treatment using 50 µg/mL of protease K (PK). For complete solubilization, mitochondria were treated
863 with 1% Triton X-100 (1% Triton) and PK and precipitated using 72% trichloroacetic acid. Samples
864 were analyzed by SDS-PAGE and western blot, using antibodies against Calnexin, Tom70, CPOX,

865 Mic60, Tim44, and FLAG-tag. **(E)** Mitochondria as in D were either sonicated in a high-salt buffer (500
866 mM NaCl pH 7.6) or subjected to carbonate extraction (100 mM Na_2CO_3 pH 10.8 or 100 mM Na_2CO_3
867 pH 11.5). Pellet (P) and supernatant (S) fractions were separated by ultracentrifugation, while
868 untreated total samples (T) served as control. Samples were analyzed by SDS-PAGE and western blot
869 using antibodies against Hsp60, Sam50, Mic60, and FLAG.

870 **Figure 5. SneRING interacts with mitochondrial and ER proteins. (A, B)** A human codon-adjusted
871 FLAG-tagged version of the SneRING was overexpressed in U2OS cells using PEI MAX® transfection.
872 24 h later, cells were infected with Sne at an MOI 1. Non-transfected cells served as control.
873 Immunoprecipitation was performed using FLAG-magnetic beads and the precipitated proteins were
874 quantified by mass spectrometry. The graphs show identified proteins, with significance ($-\log_{10}$p-
875 value) plotted against the $\log_2$ fold change ($\log_2$FC) of transfected/infected U2OS cells
876 (U2OS+Sne+SneRING) relative to non-transfected/infected controls (U2OS+Sne) **(A)** or of
877 transfected/infected U2OS cells (U2OS+Sne+SneRING) relative to transfected/non-infected controls
878 (U2OS+SneRING) **(B)**. Enriched proteins are labeled in blue, reduced proteins are shown in red, and
879 grey represents unchanged proteins. Only host cell proteins are shown.

880

881 ## Acknowledgments

882 We thank Prof. Dr. David Komander for the University of Melbourne for providing a panel of
883 deubiquitinating and E2 ubiquitin-conjugating enzymes. We thank Prof. Dr. Alexander Buchberger and
884 Prof. Dr. Martin Eilers from the University of Würzburg and Prof. Dr. Katsuyoshi Mihara from the
885 Kyushu University for antibodies. We also thank Susanne Meyer for the University of Würzburg for
886 the production of M1-linked ubiquitin chains. This study was supported by the Deutsche
887 Forschungsgemeinschaft (DFG, German Research Society) through a GRK2243/1+2 grant to VK-P.

888

889 ## Ethics statement

890 Primary cells used in this study originate from leukoreduction system cones made available by the
891 Institut für Klinische Transfusionsmedizin und Hämotherapie of the University of Würzburg, Germany
892 for research purposes and are not subject to approval by the Ethics Committee of the University of
893 Würzburg.

894

895 ## Conflict of Interest

896 The authors declare that they have no conflict of interest.

897

898 ## References

899 Akutsu M, Dikic I, Bremm A (2016) Ubiquitin chain diversity at a glance. *J Cell Sci* 129: 875-880
900 Al-Younes HM, Al-Zereini W, Obeidat NM (2017) Molecular evidence for the absence of an association
901 between Simkania negevensis and respiratory diseases. *J Med Microbiol* 66: 1324-1327
902 Ashida H, Sasakawa C (2017) Bacterial E3 ligase effectors exploit host ubiquitin systems. *Curr Opin*
903 *Microbiol* 35: 16-22
904 Berrow NS, Alderton D, Sainsbury S, Nettleship J, Assenberg R, Rahman N, Stuart DI, Owens RJ (2007)
905 A versatile ligation-independent cloning method suitable for high-throughput expression screening
906 applications. *Nucleic Acids Res* 35: e45
907 Boll V, Hermanns T, Uthoff M, Erven I, Hörner EM, Kozjak-Pavlovic V, Baumann U, Hofmann K (2023)
908 Functional and structural diversity in deubiquitinases of the Chlamydia-like bacterium Simkania
909 negevensis. *Nat Commun* 14: 7335
910 Bremm A, Freund SM, Komander D (2010) Lys11-linked ubiquitin chains adopt compact
911 conformations and are preferentially hydrolyzed by the deubiquitinase Cezanne. *Nat Struct Mol Biol*
912 17: 939-947
913 Bucher P, Karplus K, Moeri N, Hofmann K (1996) A flexible motif search technique based on
914 generalized profiles. *Comput Chem* 20: 3-23
915 Chai Q, Wang X, Qiang L, Zhang Y, Ge P, Lu Z, Zhong Y, Li B, Wang J, Zhang L *et al* (2019) A
916 Mycobacterium tuberculosis surface protein recruits ubiquitin to trigger host xenophagy. *Nat*
917 *Commun* 10: 1973
918 Chambers LR, Ye Q, Cai J, Gong M, Ledvina HE, Zhou H, Whiteley AT, Suhandynata RT, Corbett KD
919 (2024) A eukaryotic-like ubiquitination system in bacterial antiviral defence. *Nature* 631: 843-849
920 Chanput W, Mes JJ, Wichers HJ (2014) THP-1 cell line: an in vitro cell model for immune modulation
921 approach. *Int Immunopharmacol* 23: 37-45
922 Collingro A, Tischler P, Weinmaier T, Penz T, Heinz E, Brunham RC, Read TD, Bavoil PM, Sachse K,
923 Kahane S *et al* (2011) Unity in variety--the pan-genome of the Chlamydiae. *Mol Biol Evol* 28: 3253-
924 3270
925 Croxatto A, Rieille N, Kernif T, Bitam I, Aeby S, Péter O, Greub G (2014) Presence of Chlamydiales DNA
926 in ticks and fleas suggests that ticks are carriers of Chlamydiae. *Ticks Tick Borne Dis* 5: 359-365
927 Deshaies RJ, Joazeiro CA (2009) RING domain E3 ubiquitin ligases. *Annu Rev Biochem* 78: 399-434
928 Dikic I, Schulman BA (2023) An expanded lexicon for the ubiquitin code. *Nat Rev Mol Cell Biol* 24: 273-
929 287
930 Everett KD, Bush RM, Andersen AA (1999) Emended description of the order Chlamydiales, proposal
931 of Parachlamydiaceae fam. nov. and Simkaniaceae fam. nov., each containing one monotypic genus,
932 revised taxonomy of the family Chlamydiaceae, including a new genus and five new species, and
933 standards for the identification of organisms. *Int J Syst Bacteriol* 49 Pt 2: 415-440
934 Fiskin E, Bhogaraju S, Herhaus L, Kalayil S, Hahn M, Dikic I (2017) Structural basis for the recognition
935 and degradation of host TRIM proteins by Salmonella effector SopA. *Nat Commun* 8: 14004
936 French ME, Koehler CF, Hunter T (2021) Emerging functions of branched ubiquitin chains. *Cell Discov*
937 7: 6
938 Fritsche TR, Horn M, Wagner M, Herwig RP, Schleifer KH, Gautom RK (2000) Phylogenetic diversity
939 among geographically dispersed Chlamydiales endosymbionts recovered from clinical and
940 environmental isolates of Acanthamoeba spp. *Appl Environ Microbiol* 66: 2613-2619
941 Gonen H, Bercovich B, Orian A, Carrano A, Takizawa C, Yamanaka K, Pagano M, Iwai K, Ciechanover A
942 (1999) Identification of the ubiquitin carrier proteins, E2s, involved in signal-induced conjugation and
943 subsequent degradation of IkappaBalpha. *J Biol Chem* 274: 14823-14830
944 Haakonsen DL, Rape M (2019) Branching Out: Improved Signaling by Heterotypic Ubiquitin Chains.
945 *Trends Cell Biol* 29: 704-716
946 Harper JW, Ordureau A, Heo J-M (2018) Building and decoding ubiquitin chains for mitophagy. *Nat*
947 *Rev Mol Cell Biol* 19: 93-108

Hermanns T, Hofmann K (2019) Bacterial DUBs: deubiquitination beyond the seven classes. *Biochem Soc Trans* 47: 1857-1866

Hermanns T, Pichlo C, Woiwode I, Klopffleisch K, Witting KF, Ovaa H, Baumann U, Hofmann K (2018) A family of unconventional deubiquitinases with modular chain specificity determinants. *Nat Commun* 9: 799

Herweg JA, Pons V, Becher D, Hecker M, Krohne G, Barbier J, Berger H, Rudel T, Mehlitz A (2016) Proteomic analysis of the Simkania-containing vacuole: the central role of retrograde transport. *Mol Microbiol* 99: 151-171

Herweg JA, Rudel T (2016) Interaction of Chlamydiae with human macrophages. *Febs j* 283: 608-618

Hochstrasser M (2001) SP-RING for SUMO: new functions bloom for a ubiquitin-like protein. *Cell* 107: 5-8

Holm L (2022) Dali server: structural unification of protein families. *Nucleic Acids Res* 50: W210-w215

Hör J, Wolf SG, Sorek R (2024) Bacteria conjugate ubiquitin-like proteins to interfere with phage assembly. *Nature* 631: 850-856

Hospenthal MK, Mevissen TET, Komander D (2015) Deubiquitinase-based analysis of ubiquitin chain architecture using Ubiquitin Chain Restriction (UbiCRest). *Nat Protoc* 10: 349-361

Houben K, Dominguez C, van Schaik FM, Timmers HT, Bonvin AM, Boelens R (2004) Solution structure of the ubiquitin-conjugating enzyme UbcH5B. *J Mol Biol* 344: 513-526

Humphries AD, Streimann IC, Stojanovski D, Johnston AJ, Yano M, Hoogenraad NJ, Ryan MT (2005) Dissection of the mitochondrial import and assembly pathway for human Tom40. *J Biol Chem* 280: 11535-11543

Husain S, Kahane S, Friedman MG, Paterson DL, Studer S, McCurry KR, Wolf DG, Zeevi A, Pilewski J, Greenberg D (2007) Simkania negevensis in bronchoalveolar lavage of lung transplant recipients: a possible association with acute rejection. *Transplantation* 83: 138-143

Hwang J, Qi L (2018) Quality Control in the Endoplasmic Reticulum: Crosstalk between ERAD and UPR pathways. *Trends Biochem* 43: 593-605

Jamal AJ, Resende MR, Prochnow T, McGilvray I, Pilewski JM, Crespo MM, Singer LG, McCurry KR, Kolls JK, Keshavjee S *et al* (2015) Simkania negevensis and acute cellular rejection in lung transplant recipients. *Clin Transplant* 29: 705-711

Jumper J, Evans R, Pritzel A, Green T, Figurnov M, Ronneberger O, Tunyasuvunakool K, Bates R, Žídek A, Potapenko A *et al* (2021) Highly accurate protein structure prediction with AlphaFold. *Nature* 596: 583-589

Jury B, Fleming C, Huston WM, Luu LDW (2023) Molecular pathogenesis of Chlamydia trachomatis. *Front Cell Infect Microbiol* 13: 1281823

Kahane S, Dvoskin B, Friedman MG (2008) The role of monocyte/macrophages as vehicles of dissemination of Simkania negevensis: an in vitro simulation model. *FEMS Immunol Med Microbiol* 52: 219-227

Kahane S, Dvoskin B, Mathias M, Friedman MG (2001) Infection of Acanthamoeba polyphaga with Simkania negevensis and S. negevensis survival within amoebal cysts. *Appl Environ Microbiol* 67: 4789-4795

Kahane S, Fruchter D, Dvoskin B, Friedman MG (2007) Versatility of Simkania negevensis infection in vitro and induction of host cell inflammatory cytokine response. *J Infect* 55: e13-21

Kahane S, Gonen R, Sayada C, Elion J, Friedman MG (1993) Description and partial characterization of a new Chlamydia-like microorganism. *FEMS Microbiol Lett* 109: 329-333

Kahane S, Greenberg D, Friedman MG, Haikin H, Dagan R (1998) High prevalence of "Simkania Z," a novel Chlamydia-like bacterium, in infants with acute bronchiolitis. *J Infect Dis* 177: 1425-1429

Kahane S, Kimmel N, Friedman MG (2002) The growth cycle of Simkania negevensis. *Microbiology (Reading, U K)* 148: 735-742

Katoh K, Standley DM (2013) MAFFT multiple sequence alignment software version 7: improvements in performance and usability. *Mol Biol Evol* 30: 772-780

Koch RD, Hörner EM, Münch N, Maier E, Kozjak-Pavlovic V (2020) Modulation of Host Cell Death and Lysis Are Required for the Release of Simkania negevensis. *Front Cell Infect Microbiol* 10: 594932

1000 Komander D, Reyes-Turcu F, Licchesi JD, Odenwaelder P, Wilkinson KD, Barford D (2009) Molecular
1001 discrimination of structurally equivalent Lys 63-linked and linear polyubiquitin chains. *EMBO Rep* 10:
1002 466-473
1003 Kozjak-Pavlovic V, Ott C, Götz M, Rudel T (2011) Neisserial Omp85 Protein Is Selectively Recognized
1004 and Assembled into Functional Complexes in the Outer Membrane of Human Mitochondria. *J Biol*
1005 *Chem* 286: 27019-27026
1006 Kozjak V, Wiedemann N, Milenkovic D, Lohaus C, Meyer HE, Guiard B, Meisinger C, Pfanner N (2003)
1007 An essential role of Sam50 in the protein sorting and assembly machinery of the mitochondrial outer
1008 membrane. *J Biol Chem* 278: 48520-48523
1009 Krieger E, Vriend G (2014) YASARA View - molecular graphics for all devices - from smartphones to
1010 workstations. *Bioinformatics* 30: 2981-2982
1011 Kuo CC, Chen HH, Wang SP, Grayston JT (1986) Identification of a new group of Chlamydia psittaci
1012 strains called TWAR. *J Clin Microbiol* 24: 1034-1037
1013 Levin I, Eakin C, Blanc MP, Klevit RE, Miller SI, Brzovic PS (2010) Identification of an unconventional E3
1014 binding surface on the UbcH5 ~ Ub conjugate recognized by a pathogenic bacterial E3 ligase. *Proc*
1015 *Natl Acad Sci U S A* 107: 2848-2853
1016 Li CM, Kang J, Baek J, Kim Y, Park H, Jung Y-K (2024) Cytosolic FKBPL and ER-resident CKAP4 co-
1017 regulates ER-phagy and protein secretion. *Nature Commun* 15: 7886
1018 Lieberman D, Kahane S, Lieberman D, Friedman MG (1997) Pneumonia with serological evidence of
1019 acute infection with the Chlamydia-like microorganism "Z". *Am J Respir Crit Care Med* 156: 578-582
1020 Lim JY, Yoon J, Hovde CJ (2010) A brief overview of Escherichia coli O157:H7 and its plasmid O157. *J*
1021 *Microbiol Biotechnol* 20: 5-14
1022 Lin DY, Diao J, Zhou D, Chen J (2011) Biochemical and structural studies of a HECT-like ubiquitin ligase
1023 from Escherichia coli O157:H7. *J Biol Chem* 286: 441-449
1024 Liu J, Xiao Q, Xiao J, Niu C, Li Y, Zhang X, Zhou Z, Shu G, Yin G (2022) Wnt/β-catenin signalling:
1025 function, biological mechanisms, and therapeutic opportunities. *Signal Transduct Target Ther* 7: 3
1026 Livak KJ, Schmittgen TD (2001) Analysis of Relative Gene Expression Data Using Real-Time
1027 Quantitative PCR and the 2−ΔΔCT Method. *Methods* 25: 402-408
1028 Maculins T, Fiskin E, Bhogaraju S, Dikic I (2016) Bacteria-host relationship: ubiquitin ligases as
1029 weapons of invasion. *Cell Res* 26: 499-510
1030 Mehlitz A, Karunakaran K, Herweg JA, Krohne G, van de Linde S, Rieck E, Sauer M, Rudel T (2014) The
1031 chlamydial organism Simkania negevensis forms ER vacuole contact sites and inhibits ER-stress. *Cell*
1032 *Microbiol* 16: 1224-1243
1033 Merkwirth C, Langer T (2009) Prohibitin function within mitochondria: essential roles for cell
1034 proliferation and cristae morphogenesis. *Biochim Biophys Acta* 1793: 27-32
1035 Mevissen TE, Hospenthal MK, Geurink PP, Elliott PR, Akutsu M, Arnaudo N, Ekkebus R, Kulathu Y,
1036 Wauer T, El Oualid F *et al* (2013) OTU deubiquitinases reveal mechanisms of linkage specificity and
1037 enable ubiquitin chain restriction analysis. *Cell* 154: 169-184
1038 Michel MA, Elliott PR, Swatek KN, Simicek M, Pruneda JN, Wagstaff JL, Freund SM, Komander D
1039 (2015) Assembly and specific recognition of k29- and k33-linked polyubiquitin. *Mol Cell* 58: 95-109
1040 Milenkovic D, Kozjak V, Wiedemann N, Lohaus C, Meyer HE, Guiard B, Pfanner N, Meisinger C (2004)
1041 Sam35 of the mitochondrial protein sorting and assembly machinery is a peripheral outer membrane
1042 protein essential for cell viability. *J Biol Chem* 279: 22781-22785
1043 Namba T (2019) BAP31 regulates mitochondrial function via interaction with Tom40 within ER-
1044 mitochondria contact sites. *Sci Adv* 5: eaaw1386
1045 Natarajan R, Linstedt AD (2004) A cycling cis-Golgi protein mediates endosome-to-Golgi traffic. *Mol*
1046 *Biol Cell* 15: 4798-4806
1047 Nataro JP, Kaper JB (1998) Diarrheagenic Escherichia coli. *Clin Microbiol Rev* 11: 142-201
1048 Newman L, Rowley J, Vander Hoorn S, Wijesooriya NS, Unemo M, Low N, Stevens G, Gottlieb S, Kiarie
1049 J, Temmerman M (2015) Global Estimates of the Prevalence and Incidence of Four Curable Sexually
1050 Transmitted Infections in 2012 Based on Systematic Review and Global Reporting. *PLoS One* 10:
1051 e0143304

1052 Otten EG, Werner E, Crespillo-Casado A, Boyle KB, Dharamdasani V, Pathe C, Santhanam B, Randow F
1053 (2021) Ubiquitylation of lipopolysaccharide by RNF213 during bacterial infection. *Nature* 594: 111-
1054 116
1055 Pearce MM, Wormer DB, Wilkens S, Wojcikiewicz RJ (2009) An endoplasmic reticulum (ER) membrane
1056 complex composed of SPFH1 and SPFH2 mediates the ER-associated degradation of inositol 1,4,5-
1057 trisphosphate receptors. *J Biol Chem* 284: 10433-10445
1058 Quezada CM, Hicks SW, Galán JE, Stebbins CE (2009) A family of Salmonella virulence factors
1059 functions as a distinct class of autoregulated E3 ubiquitin ligases. *Proc Natl Acad Sci U S A* 106: 4864-
1060 4869
1061 Saville MK, Sparks A, Xirodimas DP, Wardrop J, Stevenson LF, Bourdon JC, Woods YL, Lane DP (2004)
1062 Regulation of p53 by the ubiquitin-conjugating enzymes UbcH5B/C in vivo. *J Biol Chem* 279: 42169-
1063 42181
1064 Scaioli E, Biondi R, Liverani E, Sartini A, Troiano A, Fuccio L, Muratori R, Lombardi G, Onorini D, Dal
1065 Monte P *et al* (2019) Simkania negevensis in Crohn's Disease. *Dig Dis Sci* 64: 3284-3290
1066 Schuepbach T, Pagni M, Bridge A, Bougueleret L, Xenarios I, Cerutti L (2013) pfsearchV3: a code
1067 acceleration and heuristic to search PROSITE profiles. *Bioinformatics* 29: 1215-1217
1068 Seufert W, Jentsch S (1990) Ubiquitin-conjugating enzymes UBC4 and UBC5 mediate selective
1069 degradation of short-lived and abnormal proteins. *Embo J* 9: 543-550
1070 Sheng X, You Q, Zhu H, Chang Z, Li Q, Wang H, Wang C, Wang H, Hui L, Du C *et al* (2017) Bacterial
1071 effector NleL promotes enterohemorrhagic E. coli-induced attaching and effacing lesions by
1072 ubiquitylating and inactivating JNK. *PLoS Pathog* 13: e1006534
1073 Smit JJ, Monteferrario D, Noordermeer SM, van Dijk WJ, van der Reijden BA, Sixma TK (2012) The E3
1074 ligase HOIP specifies linear ubiquitin chain assembly through its RING-IBR-RING domain and the
1075 unique LDD extension. *Embo J* 31: 3833-3844
1076 Steele-Mortimer O (2008) The Salmonella-containing vacuole: moving with the times. *Curr Opin*
1077 *Microbiol* 11: 38-45
1078 Stewart MD, Ritterhoff T, Klevit RE, Brzovic PS (2016) E2 enzymes: more than just middle men. *Cell*
1079 *Res* 26: 423-440
1080 Sun S, Hou H, Ma G, Ma Q, Li N, Zhang L, Dong C, Cao M, Tam KY, Ying Z *et al* (2022) The interaction
1081 between E3 ubiquitin ligase Parkin and mitophagy receptor PHB2 links inner mitochondrial
1082 membrane ubiquitination to efficient mitophagy. *J Biol Chem* 298: 102704
1083 Swatek KN, Komander D (2016) Ubiquitin modifications. *Cell Res* 26: 399-422
1084 Toma-Fukai S, Shimizu T (2021) Structural Diversity of Ubiquitin E3 Ligase. *Molecules* 26
1085 Tripathi-Giesgen I, Behrends C, Alpi AF (2021) The ubiquitin ligation machinery in the defense against
1086 bacterial pathogens. *EMBO Rep* 22: e52864
1087 UniProtConsortium (2023) UniProt: the Universal Protein Knowledgebase in 2023. *Nucleic Acids Res*
1088 51: D523-d531
1089 Vandesompele J, De Preter K, Pattyn F, Poppe B, Van Roy N, De Paepe A, Speleman F (2002) Accurate
1090 normalization of real-time quantitative RT-PCR data by geometric averaging of multiple internal
1091 control genes. *Genome Biol* 3: research0034.0031
1092 Vedrenne C, Klopfenstein DR, Hauri HP (2005) Phosphorylation controls CLIMP-63-mediated
1093 anchoring of the endoplasmic reticulum to microtubules. *Mol Biol Cell* 16: 1928-1937
1094 Vouga M, Baud D, Greub G (2017) Simkania negevensis, an insight into the biology and clinical
1095 importance of a novel member of the Chlamydiales order. *Crit Rev Microbiol* 43: 62-80
1096 Wagner F, Kunz TC, Chowdhury SR, Thiede B, Fraunholz M, Eger D, Kozjak-Pavlovic V (2019) Armadillo
1097 repeat-containing protein 1 is a dual localization protein associated with mitochondrial
1098 intermembrane space bridging complex. *PLoS One* 14: e0218303
1099 Wang T, Yin L, Cooper EM, Lai MY, Dickey S, Pickart CM, Fushman D, Wilkinson KD, Cohen RE,
1100 Wolberger C (2009) Evidence for bidentate substrate binding as the basis for the K48 linkage
1101 specificity of otubain 1. *J Mol Biol* 386: 1011-1023
1102 Wei Y, Chiang WC, Sumpter R, Jr., Mishra P, Levine B (2017) Prohibitin 2 Is an Inner Mitochondrial
1103 Membrane Mitophagy Receptor. *Cell* 168: 224-238.e210

1104 Wickliffe KE, Williamson A, Meyer HJ, Kelly A, Rape M (2011) K11-linked ubiquitin chains as novel
1105 regulators of cell division. *Trends Cell Biol* 21: 656-663
1106 Yamada A, Hikichi M, Nozawa T, Nakagawa I (2021) FBXO2/SCF ubiquitin ligase complex directs
1107 xenophagy through recognizing bacterial surface glycan. *EMBO Rep* 22: e52584
1108 Yau R, Rape M (2016) The increasing complexity of the ubiquitin code. *Nat Cell Biol* 18: 579-586
1109 Ye Y, Akutsu M, Reyes-Turcu F, Enchev RI, Wilkinson KD, Komander D (2011) Polyubiquitin binding and
1110 cross-reactivity in the USP domain deubiquitinase USP21. *EMBO Rep* 12: 350-357
1111 Yu Z, Jiang X, Qin L, Deng H, Wang J, Ren W, Li H, Zhao L, Liu H, Yan H *et al* (2021) A novel UBE2T
1112 inhibitor suppresses Wnt/β-catenin signaling hyperactivation and gastric cancer progression by
1113 blocking RACK1 ubiquitination. *Oncogene* 40: 1027-1042
1114 Zhang Y, Higashide WM, McCormick BA, Chen J, Zhou D (2006) The inflammation-associated
1115 Salmonella SopA is a HECT-like E3 ubiquitin ligase. *Mol Microbiol* 62: 786-793
1116 Zheng N, Shabek N (2017) Ubiquitin Ligases: Structure, Function, and Regulation. *Annu Rev Biochem*
1117 86: 129-157
1118 Zhu Y, Li H, Hu L, Wang J, Zhou Y, Pang Z, Liu L, Shao F (2008) Structure of a Shigella effector reveals a
1119 new class of ubiquitin ligases. *Nat Struct Mol Biol* 15: 1302-1308

1120

Figure 1

A

```
Sne A12920      IDAWNCRSCWEPIQDGPMRHNVQCNASFHLQCIETWLKN.NLSCPFCRVEVSR
Sim-KFB93       LQSWECPICFNQFED.PII.HNGCGHTLDRQCALDSIQR.YGRCPSCNLDATM
Sim-QNJ27       LKSFECAICFNQFKD.PWI.HDACGRTMDQQCILNSIQQ.LGRCPSCNLEATM
Chl-HKST.2      SEVGNCPICFNRFEN.PYI.HSGCGNTIDFACISEAVEK.FQRCPVCNENVTM
3LRQ (TRIM37)   AEVFRCFICMEKLRD.ARL.CPHCSKLCCFSCIRRWLTEQRAQCPHCRAPLQL
2CKL (RING2)    HSELMCPICLDMLKN.TMT.TKECLHRFCADCIITALRSGNKECPTCRKKLVS
```

B

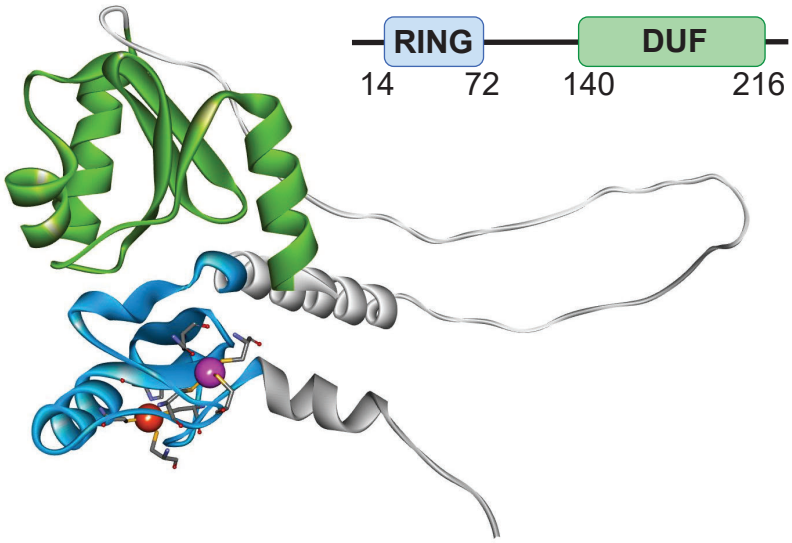

C

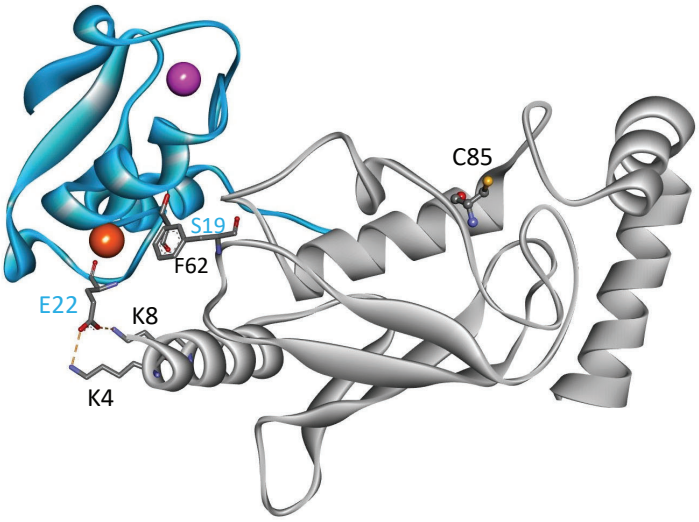

Figure 2

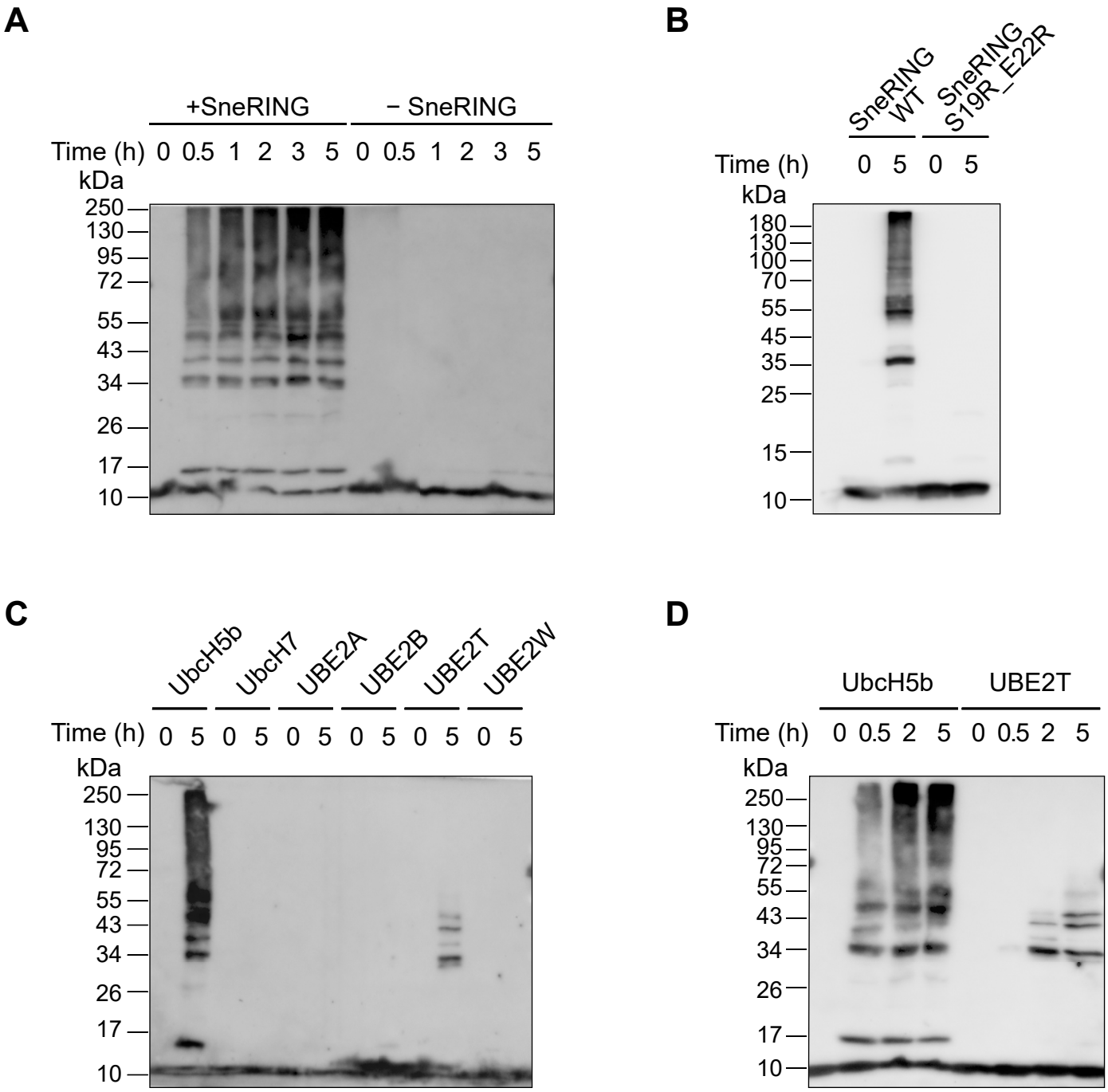
A
+SneRING
− SneRING
Time (h) 0 0.5 1 2 3 5 0 0.5 1 2 3 5
kDa
250
130
95
72
55
43
34
26
17
10
B
SneRING WT
SneRING S19R_E22R
Time (h) 0 5 0 5
kDa
180
130
100
70
55
45
35
25
15
10
C
UbcH5b
UbcH7
UBE2A
UBE2B
UBE2T
UBE2W
Time (h) 0 5 0 5 0 5 0 5 0 5 0 5
kDa
250
130
95
72
55
43
34
26
17
10
D
UbcH5b
UBE2T
Time (h) 0 0.5 2 5 0 0.5 2 5
kDa
250
130
95
72
55
43
34
26
17
10

Figure 3

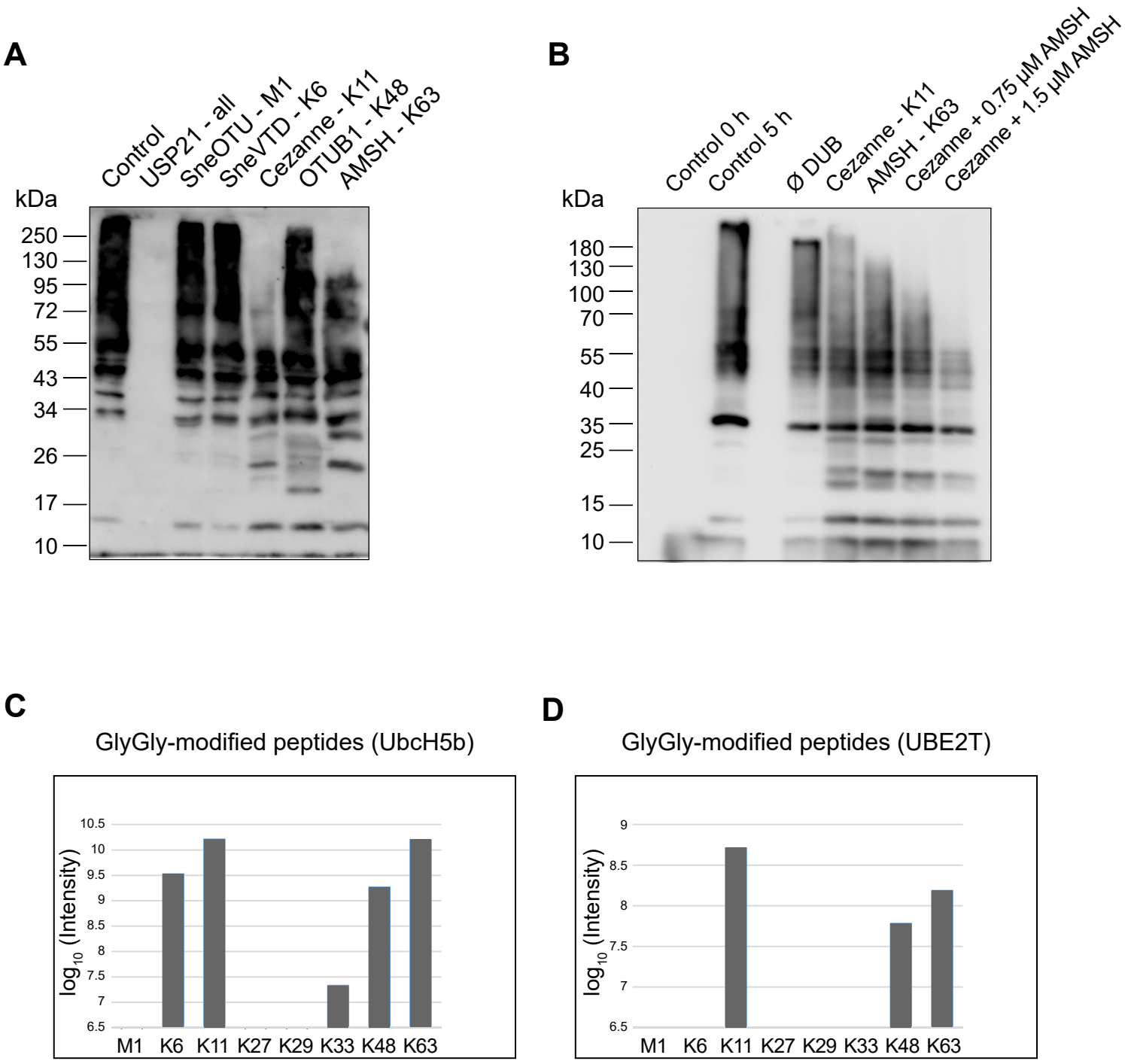
A
Control
USP21 - all
SneOTU - M1
SneVTD - K6
Cezanne - K11
OTUB1 - K48
AMSH - K63
kDa
250
130
95
72
55
43
34
26
17
10
B
Control 0 h
Control 5 h
Ø DUB
Cezanne - K11
AMSH - K63
Cezanne + 0.75 µM AMSH
Cezanne + 1.5 µM AMSH
kDa
180
130
100
70
55
40
35
25
15
10
C
GlyGly-modified peptides (UbcH5b)
log10 (Intensity)
10.5
10
9.5
9
8.5
8
7.5
7
6.5
M1 K6 K11 K27 K29 K33 K48 K63
D
GlyGly-modified peptides (UBE2T)
log10 (Intensity)
9
8.5
8
7.5
7
6.5
M1 K6 K11 K27 K29 K33 K48 K63

Figure 4

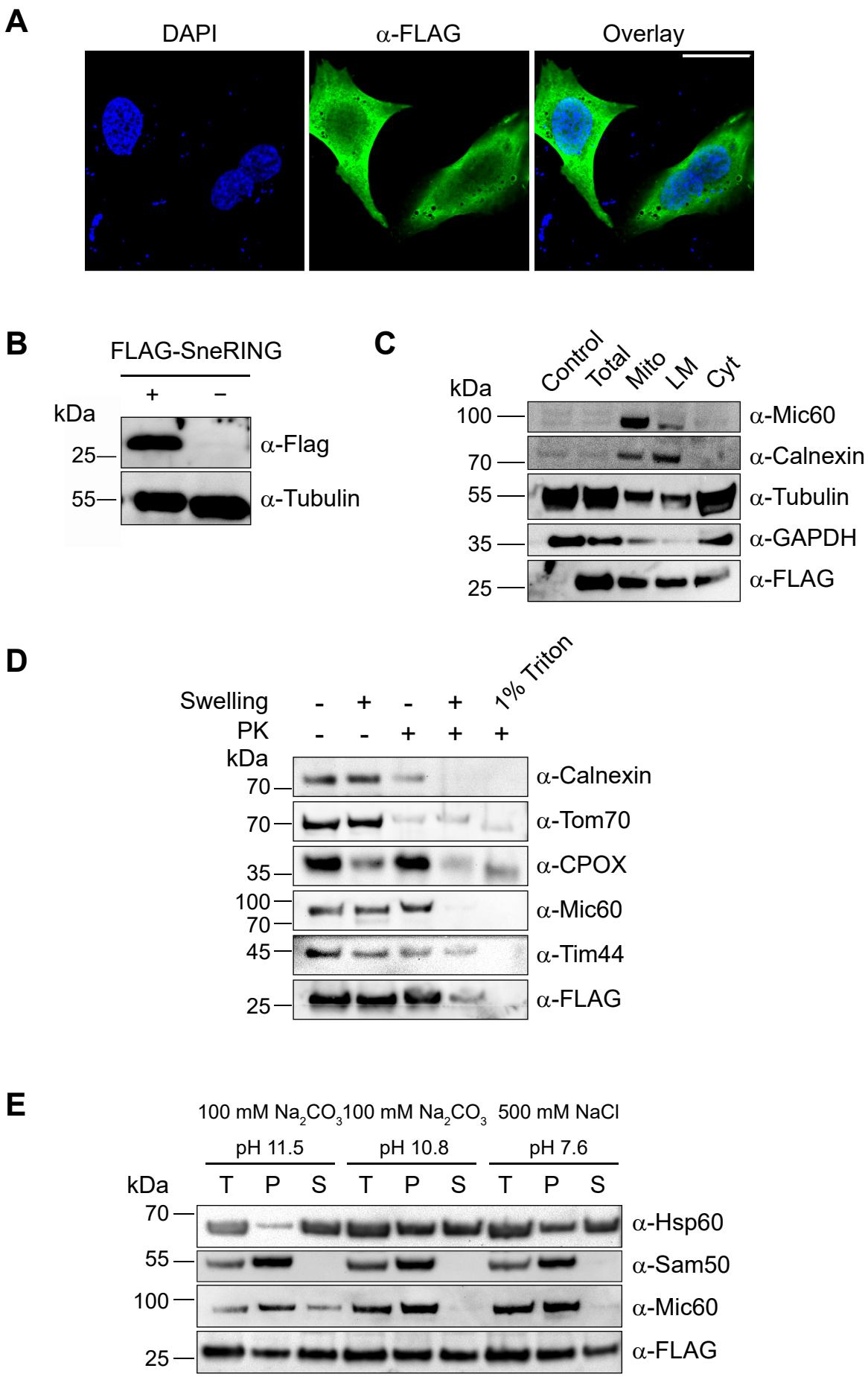
A
DAPI
α-FLAG
Overlay
B
FLAG-SneRING
+
–
kDa
25
55
α-Flag
α-Tubulin
C
Control
Total
Mito
LM
Cyt
kDa
100
70
55
35
25
α-Mic60
α-Calnexin
α-Tubulin
α-GAPDH
α-FLAG
D
Swelling - + - +
PK - - + + +
1% Triton
kDa
70
70
35
100
70
45
25
α-Calnexin
α-Tom70
α-CPOX
α-Mic60
α-Tim44
α-FLAG
E
100 mM Na2CO3 pH 11.5
100 mM Na2CO3 pH 10.8
500 mM NaCl pH 7.6
kDa
T P S T P S T P S
70
55
100
25
α-Hsp60
α-Sam50
α-Mic60
α-FLAG

Figure 5

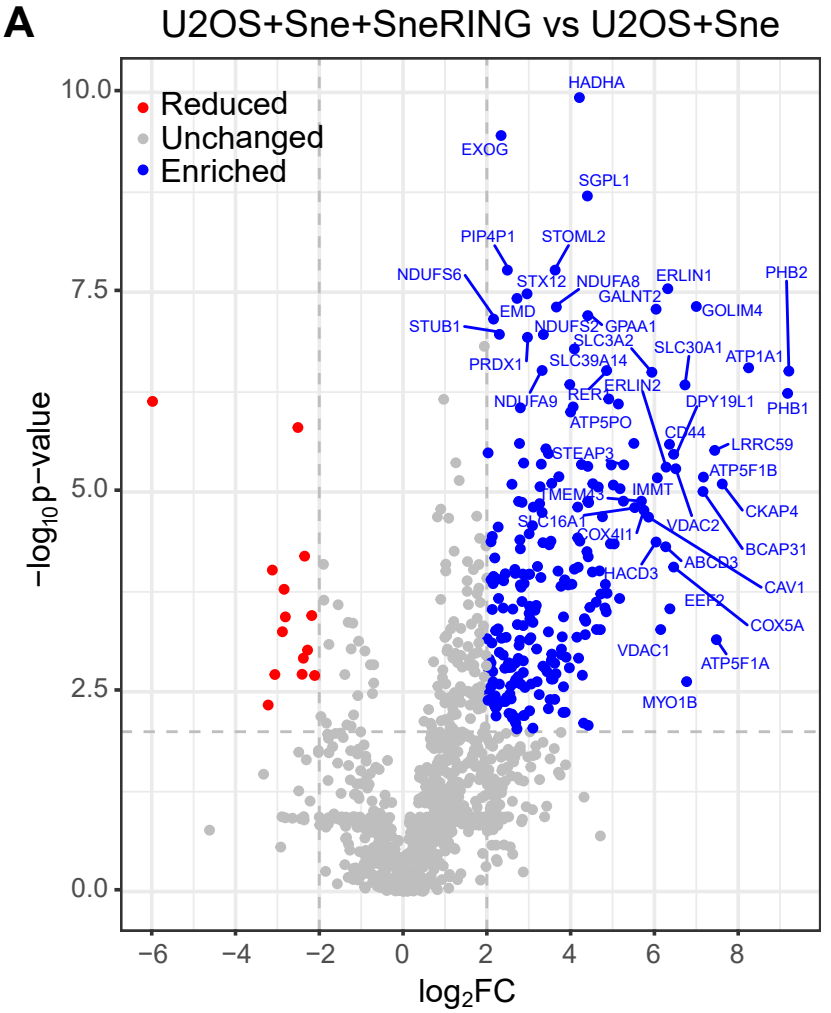
A
U2OS+Sne+SneRING vs U2OS+Sne
Reduced
Unchanged
Enriched
HADHA
EXOG
SGPL1
PIP4P1
STOML2
NDUFS6
STX12
NDUFA8
ERLIN1
PHB2
GALNT2
GOLIM4
EMD
STUB1
NDUFS2
GPAA1
SLC3A2
SLC30A1
ATP1A1
PRDX1
SLC39A14
ERLIN2
NDUFA9
RER1
DPY19L1
PHB1
ATP5PO
CD44
LRRC59
STEAP3
ATP5F1B
IMMT
TMEM43
CKAP4
SLC16A1
VDAC2
COX4I1
BCAP31
ABCD3
HACD3
CAV1
EEF2
COX5A
VDAC1
ATP5F1A
MYO1B
10.0
7.5
5.0
2.5
0.0
−6
−4
−2
0
2
4
6
8
−log10p−value
log2FC

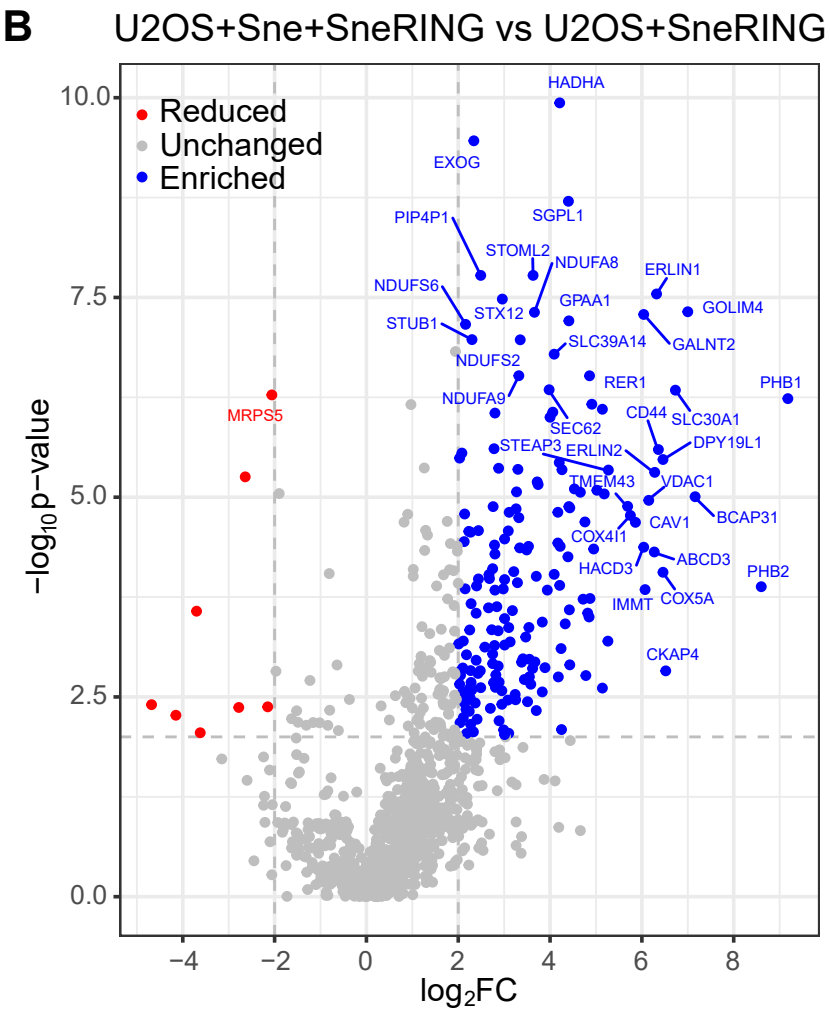
B
U2OS+Sne+SneRING vs U2OS+SneRING
Reduced
Unchanged
Enriched
HADHA
EXOG
PIP4P1
SGPL1
STOML2
NDUFA8
ERLIN1
NDUFS6
GPAA1
GOLIM4
STUB1
STX12
SLC39A14
GALNT2
NDUFS2
RER1
PHB1
NDUFA9
MRPS5
CD44
SLC30A1
SEC62
STEAP3
ERLIN2
DPY19L1
TMEM43
VDAC1
CAV1
BCAP31
COX4I1
ABCD3
HACD3
PHB2
IMMT
COX5A
CKAP4
10.0
7.5
5.0
2.5
0.0
−4
−2
0
2
4
6
8
−log10p−value
log2FC